DISCUSSION

HNF4α plays an important role in pancreatic β-cells, and mutation of this gene causes MODY1 (6). However, there has been little information available about the target genes of HNF4α in β-cells. We and others have previously reported that most of the genes involved in glucose metabolism, including *Slc2a2*, *Gck*, *Kcnj11*, *Abcc8*, and *Ins*, are not differentially expressed in βHNF4α KO islets (7, 8, 19). The present large scale expression profiling analysis also demonstrated that expression of genes known to be involved in insulin secretion was largely unchanged in HNF4α deficient islets. Like HNF4α, mutation of the HNF1α gene also causes a form of MODY (MODY3), which is characterized by β-cell dysfunction (21). Expression of many genes involved in insulin secretion, including *Slc2a2*, *Pklr*, and *Tmem27*, is decreased in HNF1α KO islets (22, 32, 33). Thus, the gene expression pattern of HNF4α KO islets differs markedly from that of HNF1α KO islets.

In the present study, we found that Anks4b gene expression was markedly reduced in both βHNF4α KO islets and HNF4α KD-MIN6 cells. Reporter gene assays and ChIP analysis demonstrated that HNF4α bound to a conserved HNF4 binding motif and activated transcription, thus indicating that Anks4b is a direct target of HNF4α in β-cells. In addition to the pancreatic islets, Anks4b is also expressed in the liver, kidney, small intestine, and colon (25). This distribution of expression is very similar to that of HNF4α, suggesting that HNF4α plays a role in Anks4b gene transcription in these tissues. Furthermore, we found that Anks4b gene expression was also regulated by HNF1α. Cotransfection of HNF4α and HNF1α dramatically stimulated promoter activity when compared with the sum of the effects of each transcription factor acting separately (Fig. 3*D*). Recently, Boj *et al.* (34) reported that HNF4α and HNF1α regulate common target genes through interdependent regulatory mechanisms. Although the mechanism of the functional interaction between HNF4α and HNF1α is still unclear, our results indicate that Anks4b gene expression is another example of such interdependent regulation.

Anks4b was originally identified as harmonin (the gene responsible for Usher deafness syndrome type 1C)-interacting protein, but its function is unknown. In this study, we showed that Anks4b binds to GRP78, a major ER chaperone protein. We also found that Anks4b knockdown significantly inhibited TG-induced CHOP expression and apoptosis in MIN6 cells, whereas Anks4b overexpression enhanced TG-induced CHOP expression and apoptosis, strongly suggesting a direct role of Anks4b in increasing the susceptibility of β-cells to ER stress and apoptosis. Investigation of Anks4b knock-out mice will improve our understanding of the role of this molecule in ER stress. Anks4b does not possess the canonical ER localization signal (35), so the molecular mechanism by which Anks4b binds to GRP78 and regulates ER stress warrants further investigation.

HNF4α plays an important role in a number of metabolic pathways, including those for gluconeogenesis, ureagenesis, fatty acid metabolism, and drug metabolism (36–38). Our finding that Anks4b is a target of HNF4α uncovers a new role for this transcription factor in regulating β-cell susceptibility to ER stress. ER stress is associated with β-cell apoptosis in common type 2 diabetes (39). Because reduced expression of Anks4b was associated with a decrease, rather than an increase, of ER stress and apoptosis, the significance of Anks4b in relation to the occurrence of MODY is unclear. However, recent genetic studies have shown that HNF4α has dual opposing roles in the β-cell during different periods of life. Although HNF4α deficiency results in diabetes in young adults (6), the same genetic defect occasionally causes hyperinsulinemic hypoglycemia at birth (40, 41). Further studies will need to address whether reduced Anks4b expression is responsible for the hypersecretion of β-cells early in life.

In conclusion, we identified Anks4b as a novel molecule that controls the susceptibility to ER stress-induced apoptosis. The ER is critical for the normal functioning of pancreatic β-cells, and ER stress-associated apoptosis is often a contributory factor to β-cell death in type 2 diabetes (39). Therefore, Anks4b may be a potential target for the treatment of diabetes associated with ER stress.

Acknowledgments—We thank Prof. J. Miyazaki (Osaka University) for the gift of MIN6 cells, Prof. T. Kitamura (Tokyo University) for providing the Plat-E cells and pMXs vector, and Dr. T. Tanaka (Tokyo University) for providing pcDNA3-HNF4α7 plasmid.

REFERENCES

1. Sladek, F. M., Zhong, W. M., Lai, E., and Darnell, J. E. (1990) Liver-enriched transcription factor HNF-4 is a novel member of the steroid hormone receptor superfamily. *Genes Dev.* **4,** 2353–2365
2. Nammo, T., Yamagata, K., Tanaka, T., Kodama, T., Sladek, F. M., Fukui, K., Katsube, F., Sato, Y., Miyagawa, J., and Shimomura, I. (2008) Expression of HNF-4α (MODY1), HNF-1β (MODY5), and HNF-1α (MODY3) proteins in the developing mouse pancreas. *Gene Expr. Patterns* **8,** 96–106
3. Hadzopoulou-Cladaras, M., Kistanova, E., Evagelopoulou, C., Zeng, S., Cladaras, C., and Ladias, J. A (1997) Functional domains of the nuclear receptor hepatocyte nuclear factor 4. *J. Biol. Chem.* **272,** 539–550
4. Ihara, A., Yamagata, K., Nammo, T., Miura, A., Yuan, M., Tanaka, T., Sladek, F. M., Matsuzawa, Y., Miyagawa, J., and Shimomura, I. (2005) Functional characterization of the HNF4α isoform (HNF4α8) expressed in pancreatic β-cells. *Biochem. Biophys. Res. Commun.* **329,** 984–990
5. Bell, G. I., and Polonsky, K. S. (2001) Diabetes mellitus and genetically programmed defects in β-cell function. *Nature* **414,** 788–791
6. Yamagata, K., Furuta, H., Oda, N., Kaisaki, P. J., Menzel, S., Cox, N. J., Fajans, S. S., Signorini, S., Stoffel, M., and Bell, G. I. (1996) Mutations in the hepatocyte nuclear factor-4α gene in maturity-onset diabetes of the young (MODY1) *Nature* **384,** 458–460
7. Miura, A., Yamagata, K., Kakei, M., Hatakeyama, H., Takahashi, N., Fukui, K., Nammo, T., Yoneda, K., Inoue, Y., Sladek, F. M., Magnuson, M. A., Kasai, H., Miyagawa, J., Gonzalez, F. J., and Shimomura, I. (2006) Hepatocyte nuclear factor-4α is essential for glucose-stimulated insulin secretion by pancreatic β-cells. *J. Biol. Chem.* **281,** 5246–5257
8. Gupta, R. K., Vatamaniuk, M. Z., Lee, C. S., Flaschen, R. C., Fulmer, J. T., Matschinsky, F. M., Duncan, S. A., and Kaestner, K. H. (2005) The MODY1 gene HNF-4α regulates selected genes involved in insulin secretion. *J. Clin. Invest.* **115,** 1006–1015
9. Hayhurst, G. P., Lee, Y. H., Lambert, G., Ward, J. M., and Gonzalez, F. J. (2001) Hepatocyte nuclear factor 4α (nuclear receptor 2A1) is essential for maintenance of hepatic gene expression and lipid homeostasis. *Mol. Cell Biol.* **21,** 1393–1403
10. Rhee, J., Inoue, Y., Yoon, J. C., Puigserver, P., Fan, M., Gonzalez, F. J., and Spiegelman, B. M. (2003) Regulation of hepatic fasting response by PPARγ coactivator-1α (PGC-1): requirement for hepatocyte nuclear factor 4α in gluconeogenesis. *Proc. Natl. Acad. Sci. U.S.A.* **100,** 4012–4017

11. Wang, H., Maechler, P., Antinozzi, P. A., Hagenfeldt, K. A., and Wollheim, C. B. (2000) Hepatocyte nuclear factor 4α regulates the expression of pancreatic β-cell genes implicated in glucose metabolism and nutrient-induced insulin secretion. *J. Biol. Chem.* **275,** 35953–35959
12. Sato, Y., Endo, H., Okuyama, H., Takeda, T., Iwahashi, H., Imagawa, A., Yamagata, K., Shimomura, I., and Inoue, M. (2011) Cellular hypoxia of pancreatic β-cells due to high levels of oxygen consumption for insulin secretion in vitro. *J. Biol. Chem.* **286,** 12524–12532
13. Miyazaki, J., Araki, K., Yamato, E., Ikegami, H., Asano, T., Shibasaki, Y., Oka, Y., and Yamamura, K. (1990) Establishment of a pancreatic β-cell line that retains glucose-inducible insulin secretion: special reference to expression of glucose transporter isoforms. *Endocrinology* **127,** 126–132
14. Yang, Q., Yamagata, K., Yamamoto, K., Cao, Y., Miyagawa, J., Fukamizu, A., Hanafusa, T., and Matsuzawa, Y. (2000) R127W-HNF-4α is a loss-of-function mutation but not a rare polymorphism and causes type II diabetes in a Japanese family with MODY1. *Diabetologia* **43,** 520–524
15. Yamagata, K., Yang, Q., Yamamoto, K., Iwahashi, H., Miyagawa, J., Okita, K., Yoshiuchi, I., Miyazaki, J., Noguchi, T., Nakajima, H., Namba, M., Hanafusa, T., and Matsuzawa, Y. (1998) Mutation P291fsinsC in the transcription factor hepatocyte nuclear factor-1α is dominant negative. *Diabetes* **47,** 1231–1235
16. Dignam, J. D., Lebovitz, R. M., and Roeder, R. G. (1983) Accurate transcription initiation by RNA polymerase II in a soluble extract from isolated mammalian nuclei. *Nucleic Acids Res.* **11,** 1475–1489
17. Shevchenko, A., Wilm, M., Vorm, O., and Mann, M. (1996) Mass spectrometric sequencing of proteins silver-stained polyacrylamide gels. *Anal. Chem.* **68,** 850–858
18. Kitamura, T., Koshino, Y., Shibata, F., Oki, T., Nakajima, H., Nosaka, T., and Kumagai, H. (2003) Retrovirus-mediated gene transfer and expression cloning: powerful tools in functional genomics. *Exp. Hematol.* **31,** 1007–1014
19. Gupta, R. K., Gao, N., Gorski, R. K., White, P., Hardy, O. T., Rafiq, K., Brestelli, J. E., Chen, G., Stoeckert, C. J., Jr., and Kaestner, K. H. (2007) Expansion of adult β-cell mass in response to increased metabolic demand is dependent on HNF-4α. *Genes Dev.* **21,** 756–769
20. Pontoglio, M., Barra, J., Hadchouel, M., Doyen, A., Kress, C., Bach, J. P., Babinet, C., and Yaniv, M. (1996) Hepatocyte nuclear factor 1 inactivation results in hepatic dysfunction, phenylketonuria, and renal Fanconi syndrome. *Cell* **84,** 575–585
21. Yamagata, K., Oda, N., Kaisaki, P. J., Menzel, S., Furuta, H., Vaxillaire, M., Southam, L., Cox, R. D., Lathrop, G. M., Boriraj, V. V., Chen, X., Cox, N. J., Oda, Y., Yano, H., Le Beau, M. M., Yamada, S., Nishigori, H., Takeda, J., Fajans, S. S., Hattersley, A. T., Iwasaki, N., Hansen, T., Pedersen, O., Polonsky, K. S., and Bell, G. I. (1996) Mutations in the hepatocyte nuclear factor-1α gene in maturity-onset diabetes of the young (MODY3) *Nature* **384,** 455–458
22. Servitja, J. M., Pignatelli, M., Maestro, M. A., Cardalda, C., Boj, S. F., Lozano, J., Blanco, E., Lafuente, A., McCarthy, M. I., Sumoy, L., Guigó, R., and Ferrer, J. (2009) Hnf1α (MODY3) controls tissue-specific transcriptional programs and exerts opposed effects on cell growth in pancreatic islets and liver. *Mol. Cell Biol.* **29,** 2945–2959
23. Ozeki, T., Takahashi, Y., Kume, T., Nakayama, K., Yokoi, T., Nunoya, K., Hara, A., and Kamataki, T. (2001) Cooperative regulation of the transcription of human dihydrodiol dehydrogenase (*DD*)*4*/aldo-keto reductase (*AKR*)*1C4* gene by hepatocyte nuclear factor (HNF)-4α/γ and HNF-1α. *Biochem. J.* **355,** 537–544
24. Eeckhoute, J., Formstecher, P., and Laine, B. (2004) Hepatocyte nuclear factor 4α enhances the hepatocyte nuclear factor 1α-mediated activation of transcription. *Nucleic Acids Res.* **32,** 2586–2593
25. Johnston, A. M., Naselli, G., Niwa, H., Brodnicki, T., Harrison, L. C., and Góñez, L. J. (2004) Harp (harmonin-interacting, ankyrin repeat-containing protein), a novel protein that interacts with harmonin in epithelial tissues. *Genes Cells* **9,** 967–982
26. Zhang, L. H., and Zhang, X. (2010) Roles of GRP78 in physiology and cancer. *Journal of cellular biochemistry* **110,** 1299–1305
27. Wang, M., Wey, S., Zhang, Y., Ye, R., and Lee, A. S. (2009) Role of the unfolded protein response regulator GRP78/BiP in development, cancer, and neurological disorders. *Antioxid. Redox Signal.* **11,** 2307–2316
28. Morris, J. A., Dorner, A. J., Edwards, C. A., Hendershot, L. M., and Kaufman, R. J. (1997) Immunoglobulin-binding protein (BiP) function is required to protect cells from endoplasmic reticulum stress but is not required for the secretion of selective proteins. *J. Biol. Chem.* **272,** 4327–4334
29. Wang, X. Z., Lawson, B., Brewer, J. W., Zinszner, H., Sanjay, A., Mi, L. J., Boorstein, R., Kreibich, G., Hendershot, L. M., and Ron, D. (1996) Signals from the stressed endoplasmic reticulum induce C/EBP-homologous protein (CHOP/GADD153). *Mol. Cell Biol.* **16,** 4273–4280
30. Treiman, M., Caspersen, C., and Christensen, S. B. (1998) A tool coming of age: thapsigargin as an inhibitor of sarco-endoplasmic reticulum Ca^{2+}-ATPases. *Trends Pharmacol. Sci.* **19,** 131–135
31. Lai, E., Teodoro, T., and Volchuk, A. (2007) Endoplasmic reticulum stress: signaling the unfolded protein response. *Physiology* **22,** 193–201
32. Fukui, K., Yang, Q., Cao, Y., Takahashi, N., Hatakeyama, H., Wang, H., Wada, J., Zhang, Y., Marselli, L., Nammo, T., Yoneda, K., Onishi, M., Higashiyama, S., Matsuzawa, Y., Gonzalez, F. J., Weir, G. C., Kasai, H., Shimomura, I., Miyagawa, J., Wollheim, C. B., and Yamagata, K. (2005) The HNF-1 target collectrin controls insulin exocytosis by SNARE complex formation. *Cell Metab.* **2,** 373–384
33. Akpinar, P., Kuwajima, S., Krützfeldt, J., and Stoffel, M. (2005) Tmem27: a cleaved and shed plasma membrane protein that stimulates pancreatic β-cell proliferation. *Cell Metab.* **2,** 385–397
34. Boj, S. F., Petrov, D., and Ferrer, J. (2010) Epistasis of transcriptomes reveals synergism between transcriptional activators Hnf1α and Hnf4α. *PLoS genet.* **6,** e1000970
35. Pagny, S., Lerouge, P., Faye, L., and Gomord, V. (1999) Signals and mechanisms for protein retention in the endoplasmic reticulum. *J. Exp. Bot.* **50,** 157–164
36. Sladek, F. M., and Seidel, S. D. (2001) in *Nuclear Receptors and Genetic Diseases* (Burris, T. P., and McCabe, E., eds) pp. 309–361, Academic Press, London, UK
37. Gonzalez, F. J. (2008) Regulation of hepatocyte nuclear factor 4α-mediated transcription. *Drug Metab. Pharmacokinet.* **23,** 2–7
38. Bolotin, E., Liao, H., Ta, T. C., Yang, C., Hwang-Verslues, W., Evans, J. R., Jiang, T., and Sladek, F. M. (2010) Integrated approach for the identification of human hepatocyte nuclear factor 4α target genes using protein binding microarrays. *Hepatology* **51,** 642–653
39. Marchetti, P., Bugliani, M., Lupi, R., Marselli, L., Masini, M., Boggi, U., Filipponi, F., Weir, G. C., Eizirik, D. L., and Cnop, M. (2007) The endoplasmic reticulum in pancreatic β-cells of type 2 diabetes patients. *Diabetologia* **50,** 2486–2494
40. Pearson, E. R., Boj, S. F., Steele, A. M., Barrett, T., Stals, K., Shield, J. P., Ellard, S., Ferrer, J., and Hattersley, A. T. (2007) Macrosomia and hyperinsulinemic hypoglycemia in patients with heterozygous mutations in the HNF4A gene. *PLoS Med.* **4,** e118
41. Kapoor, R. R., Locke, J., Colclough, K., Wales, J., Conn, J. J., Hattersley, A. T., Ellard, S., and Hussain, K. (2008) Persistent hyperinsulinemic hypoglycemia and maturity-onset diabetes of the young due to heterozygous HNF4A mutations. *Diabetes* **57,** 1659–1663

Biochemical and Biophysical Research Communications 425 (2012) 619–624

Contents lists available at SciVerse ScienceDirect

Biochemical and Biophysical Research Communications

journal homepage: www.elsevier.com/locate/ybbrc

Identification of hepatocyte growth factor activator (Hgfac) gene as a target of HNF1α in mouse β-cells

Tsuyoshi Ohki [a,b], Yoshifumi Sato [a], Tatsuya Yoshizawa [a], Ken-ichi Yamamura [c], Kentaro Yamada [b], Kazuya Yamagata [a,*]

[a] Department of Medical Biochemistry, Faculty of Life Sciences, Kumamoto University, Kumamoto, Japan
[b] Division of Endocrinology and Metabolism, Kurume University School of Medicine, Kurume, Japan
[c] Division of Developmental Genetics, Center for Animal Resources and Development, Institute of Resource Development and Analysis, Kumamoto University, Kumamoto, Japan

ARTICLE INFO

Article history:
Received 24 July 2012
Available online 1 August 2012

Keywords:
Diabetes mellitus
HNF1α
Transcription factor
Pancreatic β-cell
HGF

ABSTRACT

HNF1α is a transcription factor that is expressed in pancreatic β-cells and mutations of the HNF1α gene cause a form of monogenic diabetes. To understand the role of HNF1α in pancreatic β-cells, we established the MIN6 β-cell line that stably expressed HNF1α-specific shRNA. Expression of the gene encoding hepatocyte growth factor (HGF) activator (Hgfac), a serine protease that efficiently activates HGF, was decreased in HNF1α KD-MIN6 cells. Down-regulation of *Hgfac* expression was also found in the islets of HNF1α (+/−) mice. Reporter gene analysis and the chromatin immunoprecipitation assay indicated that HNF1α directly regulates the expression of *Hgfac* in β-cells. It has been reported that HGF has an important influence on β-cell mass and β-cell function. Thus, HNF1α might regulate β-cell mass or function at least partly by modulating Hgfac expression.

1. Introduction

HNF1α is a transcription factor that belongs to a subclass of the homeodomain family, and it is expressed in the liver, pancreas, kidney, and intestine [1,2]. HNF1α has an N-terminal dimerization domain, a DNA-binding domain with POU-like and homeodomain-like motifs, and a C-terminal transactivation domain [3]. We previously reported that heterozygous mutations of the HNF1α gene cause a form of monogenic diabetes known as maturity-onset diabetes of the young type 3 (MODY3) [4]. Clinical studies have shown that the primary cause of MODY3 is impairment of insulin secretion in response to a glucose load [5]. Mutant mice with loss of HNF1α function also develop diabetes due to impaired insulin secretion [6,7], indicating an important role of HNF1α in pancreatic β-cells. Interestingly, these mutant mice exhibit progressive reduction of β-cell numbers, suggesting that some target genes of HNF1α are also required for the maintenance of a normal β-cell mass.

To better understand the role of HNF1α in pancreatic β-cells and in the molecular mechanisms of MODY3, identification of the full spectrum of genes regulated by this factor in β-cells is necessary. Previous studies have demonstrated that *Slc2a2* (encoding glucose transporter 2 (GLUT2)), *Pklr* (encoding liver pyruvate kinase), *Tmem27* (encoding collectrin), *Hnf4a* (encoding HNF4α), and *Foxa3* (encoding HNF3γ) are direct targets of HNF1α in β-cells [8–12]. Genome-wide expression profiling has also been performed to identify additional targets of HNF1α using pancreatic islets obtained from control and HNF1α (−/−) knockout (KO) mice [13]. Although this approach revealed that expression of 5.6% of all genes was down-regulated in HNF1α KO islets, these changes might have been secondary to the onset of hyperglycemia or other effects of the diabetic state in HNF1α KO mice.

To identify the direct target genes of HNF1α in β-cells by another approach, we established the MIN6 β-cell line that stably expressed HNF1α-specific shRNA (HNF1α KD-MIN6 cells) and then compared the gene expression profile between control MIN6 cells and HNF1α KD-MIN6 cells. As a result, we demonstrated the down-regulation of several genes, including *Slc2a2*, *Tmeme27*, and *Hnf4a*, in HNF1α KD-MIN6 cells. We also found that expression of the gene encoding hepatocyte growth factor (HGF) activator (Hgfac), a serine protease that efficiently activates HGF [14], was decreased in HNF1α KD-MIN6 cells. Down-regulation of *Hgfac* expression was also found in the islets of HNF1α (+/−) mice. Reporter gene analysis and the chromatin immunoprecipitation assay confirmed that HNF1α directly regulates the expression of *Hgfac* in β-cells.

* Corresponding author. Address: Department of Medical Biochemistry, Faculty of Life Sciences, Kumamoto University, 1-1-1 Honjo, Kumamoto, Kumamoto 860-8556, Japan. Fax: +81 96 364 6940.
E-mail address: k-yamaga@kumamoto-u.ac.jp (K. Yamagata).

0006-291X/$ - see front matter © 2012 Elsevier Inc. All rights reserved.
http://dx.doi.org/10.1016/j.bbrc.2012.07.134

2. Material and methods

2.1. Cell culture

The MIN6 pancreatic β-cell line was maintained in Dulbecco's modified Eagles' medium (DMEM) (25 mM glucose) containing 10% (v/v) fetal bovine serum, 50 μM β-mercaptoethanol (β-ME), 50 U/ml penicillin, and 50 μg/ml streptomycin at 37 °C under 5% CO_2 [15]. Hela cells and Plat-E retrovirus packaging cells [16] were maintained in DMEM containing 10% (v/v) fetal bovine serum.

2.2. Retroviral infection

A specific shRNA sequence for mouse HNF1α (5′-CGAAGATGGTCAAGTCGTA-3′) was designed using the Clontech RNAi target sequence (http://bioinfo.clontech.com/). Oligonucleotides encoding shRNA were synthesized and cloned into the pSIREN-RetroQ retroviral shRNA expression vector (Clontech/Takara, Japan). Then the pSIREN-RetroQ-HNF1α vector and the negative control pSIREN-RetroQ vector were transfected into Plat-E cells using FuGENE6 (Roch, Germany). MIN6 cells were infected with either retrovirus and then selected by incubation with puromycin (5 μg/ml) to generate MIN6 cells stably expressing HNF1α shRNA (HNF1α KD-MIN6 cells) or negative control shRNA (control MIN6 cells), as described previously [17].

2.3. Quantitative RT-PCR

Total RNA was extracted by using Sepasol RNA I super reagent (Nacalai Tesque, Japan) or an RNeasy micro kit (Qiagen, CA). Quantitative real-time PCR was performed with SYBR Premix Ex Taq II (RR820A, TaKaRa) in an ABI 7300 thermal cycler (Applied Biosystems, CA). The specific primers were as follows: *Hnf1α* (5′-AAGAGCCCACAGGCGATGAG-3′ and 5′-TGGATGCACTCCGCCCTATT-3′), *Hgfac* (5′-GCACCTGCCACCTGATTGTG-3′ and 5′-GCCACGCCTCG GTACTCTGT-3′), *Slc2a2* (5′-CGTCCTACGGCTCTGGCACT-3′ and 5′-CACCCCAGCGAAGAGGAAGA-3′), *Tmem27* (5′-ATTCGGTGTGATATT TTGCATTGT-3′ and 5′-TCCAGGTGGTCCTTTGTTGTT-3′), and TATA-binding protein (*Tbp*) (5′-CCCCTTGTACCCTTCACCAAT-3′ and 5′-GAAGCTGCGGTACAATTCCAG-3′). Relative expression of each gene was normalized for that of *Tbp*.

2.4. Western blotting

Cells were lysed in RIPA buffer (50 mM Tris–HCl (pH 8.0), 150 mM NaCl, 0.1% SDS, 1% NP-40, 5 mM EDTA, 0.5% sodium deoxycholate), and 1/100 (v/v) protease inhibitor cocktail (Nacalai Tesque). Total protein was separated by SDS polyacrylamide gel electrophoresis and transferred to a polyvinylidene fluoride (PVDF) membrane (ImmobilonP; Millipore, MA), which was probed with the primary antibodies. After incubation with the secondary antibodies, proteins were visualized using Chemi-Lumi One Super (Nacalai Tesque) and a LAS-1000 imaging system (Fuji Film, Japan). The primary antibodies used in this study were anti-HNF1α (1:1000) (610902; Becton, Dickinson and Company, NJ) and anti-β-actin (1:5000) (A5441; Sigma–Aldrich, MO).

2.5. Insulin secretion

After reaching 80% confluence, MIN6 cells were plated in 24-well plates at a density of 3×10^5 cells per well. After culture for 72 h, cells were preincubated at 37 °C for 60 min in Hepes–Krebs buffer (118.4 mM NaCl, 4.7 mM KCl, 1.2 mM KH_2PO_4, 2.4 mM $CaCl_2$, 1.2 mM $MgSO_4$, 20 mM $NaHCO_3$, 2.2 mM glucose, and 10 mM Hepes) containing 0.5% (w/v) bovine serum albumin (BSA) [17]. Then the cells were incubated for 60 min in Hepes–Krebs buffer containing 22 mM glucose and insulin production was measured by using a mouse insulin ELISA kit (AKRIN-011T; Shibayagi, Japan).

2.6. Microarray analysis

Total RNA was extracted from control MIN6 cells and HNF1α KD-MIN6 cells using a miRCURY RNA isolation kit (Exiqon, Denmark) according to the manufacturer's instructions. The quality of the RNA was checked by gel electrophoresis and analysis with an Agilent 2100 Bioanalyzer (Agilent Technologies, CA). DNA microarray analysis was performed by the Toray Custom Analysis Service using the 3D-Gene™ DNA chip (Mouse Oligo chip 24K).

2.7. Isolation of pancreatic islets

HNF1α knockout mice were generated that lacked exon 1, which contains the translation start codon [K. Yamamura, and K. Yamagata, unpublished data]. HNF1α (+/−) mice showed normal glucose tolerance, as reported previously [6, and our unpublished data]. Mice were maintained with a 12 h light–12 h dark cycle and were allowed free access to food and water. These experiments were conducted according to the guidelines of the Institutional Animal Committee of Kumamoto University. Islets were isolated from the harvested pancreata of 20-week-old male HNF1α (+/−) mice ($n = 4$) and control HNF1α (+/+) littermates ($n = 4$) by collagenase digestion, as described previously [7].

2.8. Transient transfection and luciferase reporter assay

A 135 bp fragment of the mouse Hgfac gene promoter containing the putative HNF1α-binding site (−135 to −1 relative to the translation start codon when A is numbered as +1) was amplified by PCR using the primers 5′-GCTAGCGGCTGTGGAGGAGCCTAACAGGAT-3′ (underlined nucleotides indicate the cloned NheI site) and 5′-AAGCTTGGCTCCTCCTGAGCTGGCGTGAGG-3′ (underlined nucleotides indicate the cloned HindIII site), and then was subcloned into the pGL3 basic reporter (Promega, WI) to generate pGL3-Hgfac. The HNF1α-binding site was altered to 5′-GGTCGGCCCTTATCA-3′ by PCR-based mutagenesis. The pcDNA3.1-wild-type (WT)-HNF1α and pcDNA3.1-P291fsinsC-HNF1α expression plasmids have been described previously [8]. Hela cells (1.5×10^5 cells/well) or MIN6 cells (3×10^5 cells/well) were seeded into 12-well plates at 18 h before transient transfection was performed using X-treme GENE (Roche) according to the manufacturer's instructions. At 48 h after transfection, luciferase activity was measured by using a Dual-Luciferase Reporter assay system (Promega).

2.9. Chromatin immunoprecipitation (ChIP) assay

MIN6 cells were cross-linked with 1% formaldehyde for 10 min at room temperature. Then the ChIP assay was performed as described previously [17] using an anti-HNF1 antibody (sc-8986, Santa Cruz Biotechnology, CA). Immunoprecipitated DNA was amplified by real-time PCR with specific primers for the promoter region of *Hgfac* containing the HNF1α-binding motif (5′-GGCTGTG GAGGAGCCTAACAGGAT-3′ and 5′-GGCTCCTCCTGAGCTGGCGT-GAGG-3′) (P1), as well as primers for the 10 kb upstream region from the *Hgfac* translation start codon (5′-GGGCTGGGGT GC TTCGGGTA-3′ and 5′-GACCCTCCAGCGGATGGC TCA-3′) (P2), the 5.3 kb downstream region from the *Hgfac* translation start (5′-GCTGTGCTGTCCGCTCCCAG-3′ and 5′-CATGTGGCCCCAGCCTGCAA-3′) (P3), and the promoter region of *Tbp* (5′-ATCAGATGTGCGT-CAGGCGTT-3′ and 5′-TGCGGAGAAAATGACGCGA-3′) (P4). All PCR

reactions were done by using SYBR Premix Ex Taq II (TaKaRa) in an ABI 7300 thermal cycler (Applied Biosystems).

2.10. Statistical analysis

The significance of differences was assessed with the unpaired *t*-test, and $p < 0.05$ was considered to indicate statistical significance.

3. Results

3.1. Establishment of HNF1α KD-MIN6 cells and microarray analysis

In order to identify novel target genes for HNF1α in pancreatic β-cells, we established MIN6 β-cells that stably expressed HNF1α-specific shRNA (HNF1α KD-MIN6) by retroviral infection. Suppression of endogenous HNF1α expression by shRNA was confirmed at both the mRNA level (39.8% of control, $p = 0.019$) and the protein level (30.6% of control, $p = 0.007$) (Fig. 1A and B). *Slc2a2* and *Tmem27* are direct targets of HNF1α in β-cells [10,11], and expression of both these genes was significantly decreased in HNF1α KD-MIN6 cells (Fig. 1C). Loss of the function of HNF1α leads to impairment of glucose-stimulated insulin secretion by pancreatic β-cells [6,7]. Therefore, we examined insulin secretion by HNF1α KD-MIN6 cells and control MIN6 cells. Insulin secretion by HNF1α KD-MIN6 cells subjected to stimulation with 22 mM glucose was significantly decreased ($p < 0.001$) to 39.2% of that for control cells (Fig. 1D). Suppression of HNF1α expression also reduced insulin secretion by HNF1α KD-MIN6 cells in response to a low glucose concentration (decreased by 41.4%, $p < 0.001$). These results indicate that HNF1α KD-MIN6 cells can be used as a novel cellular model of MODY3.

In order to identify novel target genes of HNF1α in pancreatic β-cells, DNA microarray analysis was performed using control cells and HNF1α KD-MIN6 cells. Microarray analysis identified the down-regulation of 53 genes (0.22% of all expressed genes), which was defined as a signal log ratio $\leqslant -1.5$, in HNF1α KD-MIN6 cells and up-regulation of 38 genes (0.15% of all expressed genes), which was defined as a signal log ratio $\geqslant 2$ (Table 1 and Supplementary Table 1). Several known targets of HNF1α (*Slc2a2*, *Tmem27*, and *Hnf4α*) were found in the group of down-regulated genes.

3.2. Hgfac expression in β-cells is regulated by HNF1α

Microarray analysis revealed that expression of the gene encoding hepatocyte growth factor activator (HGFA) was reduced to 25.2% of the control level in HNF1α KD-MIN6 cells (Table 1). Down-regulation of *Hgfac* expression in HNF1α KD-MIN6 cells to 18.7% of the control level ($p < 0.001$) was confirmed by quantitative RT-PCR (Fig. 2A). HNF1α (+/−) mice were reported to be useful for investigating HNF1α-dependent transcription in pancreatic islets [18]. As shown in Fig. 2B, Hgfac mRNA expression was significantly decreased in the islets of HNF1α (+/−) mice to 45.8% of the control level ($p < 0.001$), indicating that *Hgfac* gene transcription is regulated by HNF1α *in vivo* as well as *in vitro*.

Screening of the promoter region of the mouse *Hgfac* gene by using a genomic databank revealed an HNF1α-binding site (nucleotides −83 to −97 relative to the translation start codon when *A* is designated as +1), and this binding site was also confirmed to exist in the human HGFAC gene (Fig. 2C). We cloned a 135 bp fragment

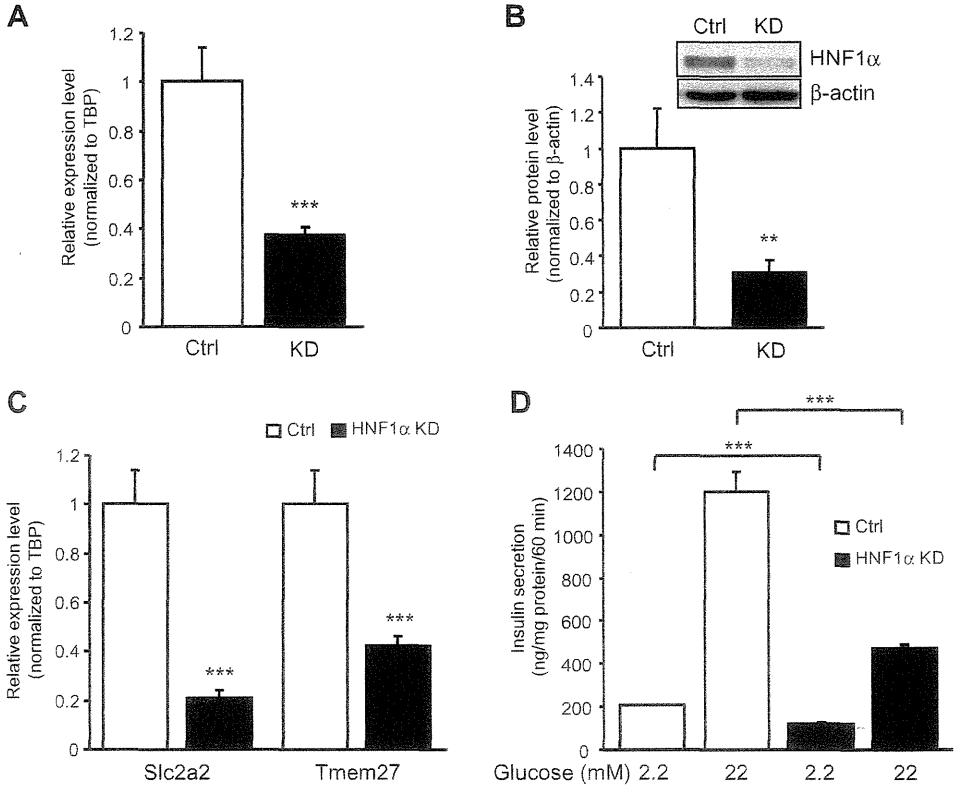

Fig. 1. Gene expression and insulin secretion by HNF1α KD-MIN6 cells. (A) Expression of HNF1α mRNA by control cells (Ctrl) ($n = 3$) and HNF1α KD-MIN6 cells (KD) ($n = 3$). Expression is normalized for that of Tbp. (B) HNF1α protein expression in HNF1α KD-MIN6 cells evaluated by Western blotting ($n = 3$). β-actin was used as the loading control. (C) Expression of Slc2a2 and Tmem27 mRNA was significantly decreased in HNF1α KD-MIN6 cells ($n = 3$). (D) Insulin secretion after exposure to glucose was decreased in HNF1α KD-MIN6 cells ($n = 4$). Data are the mean ± SD (**$p < 0.01$, ***$p < 0.001$).

Table 1
Gene list of the down-regulated genes in HNF1α KD-MIN6 cells.

Gene symbol	Gene title	Log ratio	RefSeq transcript ID
Gc	Group specific component	−3.76	NM_008096
Ugt1a6a	UDP glucuronosyltransferase 1 family, polypeptide A7C	−3.68	NM_145079
Slc2a2	Solute carrier family 2 (facilitated glucose transporter), member 2	−3.61	NM_031197
Crp	C-reactive protein, pentraxin-related	−3.48	NM_007768
Ttr	Transthyretin	−3.23	NM_013697
Tmed6	Transmembrane emp24 protein transport domain containing 6	−3.02	NM_025458
Serpina1c	Serine (or cysteine) peptidase inhibitor, clade A, member 1a	−2.90	NM_009245
Iyd	Iodotyrosine deiodinase	−2.80	NM_027391
Slc40a1	Solute carrier family 40 (iron-regulated transporter), member 1	−2.70	NM_016917
Ang1	Angiogenin, ribonuclease A family, member 1	−2.70	NM_007447
Spon2	Spondin 2, extracellular matrix protein	−2.64	NM_133903
Rnase4	Ribonuclease, RNase A family 4	−2.62	NM_021472
Golt1a	Golgi transport 1 homolog A (S. cerevisiae)	−2.53	NM_026680
Serpina1c	Serine (or cysteine) peptidase inhibitor, clade A, member 1a	−2.50	NM_009243
Serpina1d	Serine (or cysteine) peptidase inhibitor, clade A, member 1d	−2.44	NM_009246
Serpina1e	Serine (or cysteine) peptidase inhibitor, clade A, member 1e	−2.33	NM_009247
Guca1a	Guanylate cyclase activator 1a (retina)	−2.29	NM_008189
Nmbr	Neuromedin B receptor	−2.29	NM_008703
Tmem27	Transmembrane protein 27	−2.26	NM_020626
Ang4	Angiogenin, ribonuclease A family, member 4	−2.24	NM_177544
Ang5	Angiogenin, ribonuclease A family, member 5	−2.21	NM_007448
Dpp4	Dipeptidylpeptidase 4	−2.20	NM_010074
Ldha	Lactate dehydrogenase A	−2.11	NM_010699
St6gal1	Beta galactoside alpha 2,6 sialyltransferase 1	−2.05	NM_145933
Hgfac	Hepatocyte growth factor activator	−1.99	NM_019447
Pcsk9	Proprotein convertase subtilisin/kexin type 9	−1.98	NM_153565
Ang5	Angiogenin, ribonuclease A family, member 5	−1.97	NM_007448
Abcg2	ATP-binding cassette, sub-family G (WHITE), member 2	−1.96	NM_011920
Ins1	Insulin I	−1.92	NM_008386
Kif12	Kinesin family member 12	−1.89	NM_010616
Ppp1r1a	Protein phosphatase 1, regulatory (inhibitor) subunit 1A	−1.87	NM_021391
Itga6	Integrin alpha 6	−1.84	NM_008397
Myo15b	Myosin XVB	−1.84	XM_203357
Il20rb	Interleukin 20 receptor beta	−1.83	XM_358706
Degs2	Degenerative spermatocyte homolog 2 (Drosophila), lipid desaturase	−1.81	NM_027299
Tff3	Trefoil factor 3, intestinal	−1.75	NM_011575
Cpn1	Carboxypeptidase N, polypeptide 1	−1.71	NM_030703
Cbs	Cystathionine beta-synthase	−1.71	NM_144855
Insl5	Insulin-like 5	−1.70	NM_011831
Slc16a3	Solute carrier family 16 (monocarboxylic acid transporters), member 3	−1.70	NM_030696
Mbl2	Mannose binding lectin (protein C)	−1.68	NM_010776
Tm4sf4	Transmembrane 4 superfamily member 4	−1.67	NM_145539
Dact2	Dapper homolog 2, antagonist of beta-catenin (xenopus)	−1.63	NM_172826
Dscr1l1	Down syndrome critical region gene 1-like 1	−1.63	NM_030598
Anks4b	Ankyrin repeat and sterile alpha motif domain containing 4B	−1.61	NM_028085
Cacna1 h	Calcium channel, voltage-dependent, T type, alpha 1H subunit	−1.60	NM_021415
Il6ra	Interleukin 6 receptor, alpha	−1.59	NM_010559
Hnf4a	Hepatic nuclear factor 4, alpha	−1.59	NM_008261
Defb1	Defensin beta 1	−1.58	NM_007843
Sgk2	Serum/glucocorticoid regulated kinase 2	−1.56	NM_013731
Sct	Secretin	−1.52	NM_011328
Lgals2	Lectin, galactose-binding, soluble 2	−1.52	NM_025622
Nek6	NIMA (never in mitosis gene a)-related expressed kinase 6	−1.51	NM_021606

of the promoter region upstream of a luciferase reporter gene, and co-expressed it with the HNF1α expression vector in HeLa cells. We found that induction of HNF1α increased *Hgfac* promoter activity to 23.6 times the control level ($p < 0.001$) (Fig. 2D). HNF1α also activated the reporter gene by 3.1-fold ($p < 0.001$) in MIN6 cells, while dominant negative P291fsinsC-HNF1α (a frameshift mutation in the transactivation domain) [8] decreased reporter gene activity to 41.0% of the control level ($p < 0.001$) (Fig. 2E). Mutation of the putative HNF1α-binding site in the reporter gene significantly reduced transcriptional activation by HNF1α (87.3% decrease, $p < 0.001$) (Fig. 2F).

In order to investigate binding of HNF1α to the Hgfac promoter, the chromatin immunoprecipitation (ChIP) assay was performed. Cross-linked chromatin was precipitated with HNF1 antibody, after which the precipitated DNA was analyzed by PCR using primer sets that amplified the promoter region of *Hgfac* containing the putative HNF1α-binding site (P1), the 10 kb upstream region from P1 (P2), the 5.3 kb downstream region from P1 (exon 12) (P3), and the promoter region of *Tbp* (P4). As shown in Fig. 2G, specific binding of HNF1α to the promoter region (P1) was identified in MIN6 cells. These findings indicated that the *Hgfac* gene is directly regulated by HNF1α.

4. Discussion

HGF was originally identified as a potent mitogen for hepatocytes [19], but subsequent studies have shown that it has mitogenic and prosurvival effects on various cells including β-cells. Transgenic overexpression of HGF in pancreatic β-cells increases β-cell replication, mass, and function [20]. Loss of HGF signaling in β-cells during gestation leads to decreased replication and a

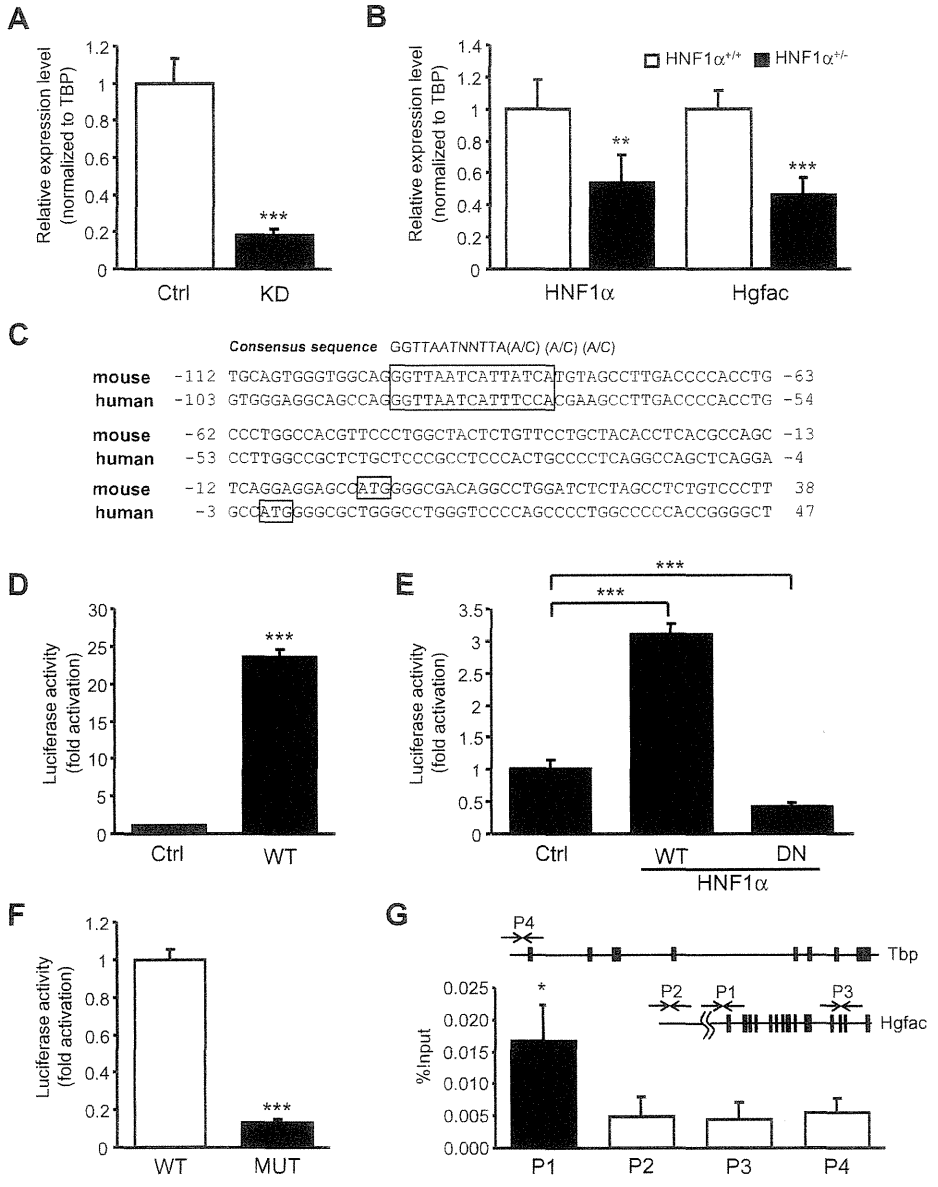

Fig. 2. Transcriptional regulation of *Hgfac* by HNF1α. (A) Expression of Hgfac mRNA by control (Ctrl) cells ($n = 3$) and HNF1α KD-MIN6 cells (KD) ($n = 3$). Expression is normalized for that of Tbp. (B) Expression of HNF1α and Hgfac mRNA in HNF1α (+/+) ($n = 4$) and HNF1α (+/−) islets ($n = 4$). (C) DNA sequences of the mouse and human Hgfac genes. The putative HNF1α-binding site is shown by a box. (D) HeLa cells were cotransfected with 800 ng of the pcDNA3.1-HNF1α expression vector as well as 200 ng of the pGL3-Hgfac reporter vector and 1 ng of pRL-TK. (E) MIN6 cells were cotransfected with 800 ng of the pcDNA3.1-HNF1α (WT) or the pcDNA3.1-P291fsinsC-HNF1α (DN) expression vector as well as 200 ng of the pGL3-Hgfac reporter vector and 0.4 ng of pRL-TK. (F) MIN6 cells were cotransfected with 800 ng of the pcDNA3.1-HNF1α (WT) expression vector as well as 200 ng of the pGL3-Hgfac (WT) or pGL3-Hgfac-mutant (MUT) reporter vector and 0.4 ng of pRL-TK. (G) Chromatin immunoprecipitation assay with MIN6 cells. PCR was performed using 4 different primer sets (P1–P4). The P2–4 regions lack the HNF1α-binding motif. Interaction of HNF1α with the P1 region of *Hgfac* was observed. Data are the mean ± SD ($^{*}p < 0.05$, $^{**}p < 0.01$, $^{***}p < 0.001$).

decline of β-cell mass, and loss of HGF signaling also accelerates the onset of diabetes in response to multiple low-dose injections of streptozotocin [21,22]. These data strongly suggest that HGF has an important influence on β-cell mass and β-cell function.

HGF is secreted in a latent form, and proteolytic conversion by the serine protease HGF activator (Hgfac) is required for its activation [14]. In this study, we found that Hgfac expression was markedly decreased in both HNF1α KD-MIN6 cells and islets from HNF1α (+/−) mice. The reporter and ChIP assays demonstrated that HNF1α bound to the conserved binding site of the *Hgfac* promoter and that it activated transcription of this gene, indicating that *Hgfac* is a direct target of HNF1α in β-cells. Although the molecular mechanisms underlying MODY3 are still unknown, HNF1α (−/−) mice and transgenic mice expressing the naturally occurring dominant negative form of human HNF1α (P291fsinsC) in their β-cells exhibit progressive reduction of β-cell mass and β-cell proliferation, indicating that HNF1α is required to maintain the β-cell mass [6,7]. Reduction of *Hgfac* gene expression and a consequent decrease of HGF signaling in β-cells might occur in HNF1α mutant mice as well as in patients with MODY3. It is possible that HNF1α controls β-cells mass at least partly by regulating cellular Hgfac expression. Investigation of β-cell specific Hgfac knockout mice could improve our understanding of how a reduction of HNF1α activity leads to a decline of β-cell mass and the onset of diabetes.

In conclusion, we established a novel cellular model of MODY3, HNF1α KD-MIN6 cells, and we identified many genes that were down-regulated in these cells. Further investigation of HNF1α KD-MIN6 cells could be useful to identify novel target genes of HNF1α in β-cells.

Acknowledgments

We thank Prof. Miyazaki (Osaka University) for the kind gift of MIN6 cells, and Prof. T. Kitamura (Tokyo University) for providing Plat-E cells. This work was supported by a Grant-in-Aid for Scientific Research (S), a Grant-in-Aid for Scientific Research on Innovative Areas, Health Labour Sciences Research Grant, and Grants from the Takeda Science Foundation, Novo Nordisk Insulin Research Foundation, Banyu Life Science Foundation International, and Japan Diabetes Foundation.

Appendix A. Supplementary data

Supplementary data associated with this article can be found, in the online version, at http://dx.doi.org/10.1016/j.bbrc.2012.07.134.

References

[1] D.B. Mendel, G.R. Crabtree, HNF-1, a member of a novel class of dimerizing homeodomain proteins, J. Biol. Chem. 266 (1991) 677–680.
[2] T. Nammo, K. Yamagata, R. Hamaoka, Q. Zhu, T. Akiyama, F. Gonzalez, J. Miyagawa, Y. Matsuzawa, Expression profile of MODY3/HNF-1α protein in the developing mouse pancreas, Diabetologia 45 (2002) 1142–1153.
[3] M. Frain, G. Swart, P. Monaci, A. Nicosia, S. Stilmpfli, R. Frank, R. Cortese, The liver-specific transcription factor LF-B1 contains a highly diverged homeobox DNA binding domain, Cell 59 (1989) 145–157.
[4] K. Yamagata, N. Oda, P.J. Kaisaki, S. Menzel, H. Furuta, M. Vaxillaire, L. Southam, R.D. Cox, G.M. Lathrop, V.V. Boriraj, X. Chen, N.J. Cox, Y. Oda, H. Yano, M.M. Le Beau, S. Yamada, H. Nishigori, J. Takeda, S.S. Fajans, A.T. Hattersleystar, N. Iwasaki, T. Hansen, O. Pedersen, K.S. Polonsky, R.C. Turner, G. Velho, J-C. Chèvreparallel, P. Froguel, G.I. Bell, Mutations in the hepatocyte nuclear factor-1α gene in maturity-onset diabetes of the young (MODY3), Nature 384 (1996) 455–458.
[5] M.M. Byrne, J. Sturis, S. Menzel, K. Yamagata, S.S. Fajans, M.J. Dronsfield, S.C. Bain, A.T. Hattersley, G. Velho, P. Froguel, G.I. Bell, K.S. Polonsky, Altered insulin secretory responses to glucose in diabetic and nondiabetic subjects with mutations in the diabetes susceptibility gene MODY3 on chromosome 12, Diabetes 45 (1996) 1503–1510.
[6] M. Pontoglio, S. Sreenan, M. Roe, W. Pugh, D. Ostrega, A. Doyen, A.J. Pick, A. Baldwin, G. Velho, P. Froguel, M. Levisetti, S. Bonner-Weir, G.I. Bell, M. Yaniv, K.S. Polonsky, Defective insulin secretion in hepatocyte nuclear factor 1α-deficient mice, J. Clin. Invest. 101 (1998) 2215–2222.
[7] K. Yamagata, T. Nammo, M. Moriwaki, A. Ihara, K. Iizuka, Q. Yang, T. Satoh, M. Li, R. Uenaka, K. Okita, H. Iwahashi, Q. Zhu, Y. Cao, A. Imagawa, Y. Tochino, T. Hanafusa, J. Miyagawa, Y. Matsuzawa, Mutant hepatocyte nuclear factor-1α in pancreatic β-cells causes abnormal islet architecture with decreased expression of E-cadherin, reduced β-cell proliferation, and diabetes, Diabetes 51 (2002) 114–123.
[8] K. Yamagata, Q. Yang, K. Yamamoto, H. Iwahashi, J. Miyagawa, K. Okita, I. Yoshiuchi, J. Miyazaki, T. Noguchi, H. Nakajima, M. Namba, T. Hanafusa, Y. Matsuzawa, Mutation P291fsinsC in the transcription factor hepatocyte nuclear factor-1α is dominant negative, Diabetes 47 (1998) 1231–1235.
[9] H. Wang, P. Maechler, K.A. Hagenfeldt, C.B. Wollheim, Dominant-negative suppression of HNF-1α function results in defective insulin gene transcription and impaired metabolism-secretion coupling in a pancreatic β-cell line, EMBO J. 17 (1998) 6701–6713.
[10] S.F. Boj, M. Parrizas, M.A. Maestro, J. Ferrer, A transcription factor regulatory circuit in differentiated pancreatic cells, Proc. Natl. Acad. Sci. USA 98 (2001) 14481–14486.
[11] K. Fukui, Q. Yang, Y. Cao, N. Takahashi, H.H. Atakeyama, H. Wang, J. Wada, Y. Zhang, L. Marselli, T. Nammo, K. Yoneda, M. Onishi, S. Higashiyama, Y. Matsuzawa, F.J. Gonzalez, G.C. Weir, H. Kasai, I. Shimomura, J. Miyagawa, C.B. Wollheim, K. Yamagata, The HNF-1 target collectrin controls insulin exocytosis by SNARE complex formation, Cell Metab. 2 (2005) 373–384.
[12] P. Akpinar, S. Kuwajima, J. Krützfeldt, M. Stoffel, Tmem27: a cleaved and shed plasma membrane protein that stimulates pancreatic beta cell proliferation, Cell Metab. 2 (2005) 385–397.
[13] J.M. Servitja, M. Pignatelli, M.A. Maestro, C. Cardalda, S.F. Boj, J. Lozano, E. Blanco, A. Lafuente, M.I. McCarthy, L. Sumoy, R. Guigó, J. Ferrer, Hnf1α (MODY3) controls tissue-specific transcriptional programs and exerts opposed effects on cell growth in pancreatic islets and liver, Mol. Cell Biol. 29 (2009) 2945–2959.
[14] K. Miyazawa, Hepatocyte growth factor activator (HGFA): a serine protease that links tissue injury to activation of hepatocyte growth factor, FEBS J. 277 (2010) 2208–2214.
[15] J. Miyazaki, K. Araki, E. Yamato, H. Ikegami, T. Asano, Y. Shibasaki, Y. Oka, K. Yamamura, Establishment of a pancreatic beta cell line that retains glucose-inducible insulin secretion: special reference to expression of glucose transporter isoforms, Endocrinology 127 (1990) 126–132.
[16] T. Kitamura, Y. Koshino, F. Shibata, T. Oki, H. Nakajima, T. Nosaka, H. Kumagai, Retrovirus-mediated gene transfer and expression cloning: powerful tools in functional genomics, Exp. Hematol. 31 (2003).1007–1014.
[17] Y. Sato, M. Hatta, M.F. Karim, T. Sawa, F.Y. Wei, S. Sato, M.A. Magnuson, F.J. Gonzalez, K. Tomizawa, T. Akaike, T. Yoshizawa, K. Yamagata, Anks4b, a novel target of HNF4α protein interacts with GRP78 protein and regulates endoplasmic reticulum stress-induced apoptosis in pancreatic β-cells, J. Biol. Chem. 287 (2012) 23236–23245.
[18] S.F. Boj, D. Petrov, J. Ferrer, Epistasis of transcriptomes reveals synergism between transcriptional activators Hnf1α and Hnf4α, PLoS Genetics 6 (2010) e1000970.
[19] T. Nakamura, T. Nishizawa, M. Hagiya, T. Seki, M. Shimonishi, A. Sugimura, K. Tashiro, S. Shimizu, Molecular cloning and expression of human hepatocyte growth factor, Nature 342 (1989) 440–443.
[20] A. Garcia-Ocaña, K.K. Takane, M.A. Syed, W.M. Philbrick, R.C. Vasavada, A.F. Stewart, Hepatocyte growth factor overexpression in the islet of transgenic mice increases beta cell proliferation, enhances islet mass, and induces mild hypoglycemia, J. Biol. Chem. 275 (2000) 1226–1232.
[21] J. Mellado-Gil, T.C. Rosa, C. Demirci, J.A. Gonzalez-Pertusa, S. Velazquez-Garcia, S. Ernst, S. Valle, R.C. Vasavada, A.F. Stewart, L.C. Alonso, A. Garcia-Ocan-a, Disruption of hepatocyte growth factor/c-Met signaling enhances pancreatic beta-cell death and accelerates the onset of diabetes, Diabetes 60 (2011) 525–536.
[22] C. Demirci, S. Ernst, J.C. Alvarez-Perez, T. Rosa, S. Valle, V. Shridhar, G.P. Casinelli, L.C. Alonso, R.C. Vasavada, A. García-Ocana, Loss of HGF/c-Met signaling in pancreatic β-cells leads to incomplete maternal β-cell adaptation and gestational diabetes mellitus, Diabetes 61 (2012) 1143–1152.

FEBS Letters 586 (2012) 4215–4222

FEBS Letters

journal homepage: www.FEBSLetters.org

Novel function of transthyretin in pancreatic alpha cells

Yu Su [a], Hirofumi Jono [a,e,f,*], Yohei Misumi [b], Takafumi Senokuchi [c], Jianying Guo [a], Mitsuharu Ueda [a], Satoru Shinriki [a], Masayoshi Tasaki [a], Makoto Shono [a], Konen Obayashi [a], Kazuya Yamagata [d], Eiichi Araki [c], Yukio Ando [a]

[a] Department of Diagnostic Medicine, Graduate School of Medical Sciences, Kumamoto University Hospital, Kumamoto, Japan
[b] Department of Neurology, Graduate School of Medical Sciences, Kumamoto University Hospital, Kumamoto, Japan
[c] Department of Metabolic Medicine, Graduate School of Medical Sciences, Kumamoto University Hospital, Kumamoto, Japan
[d] Department of Medical Biochemistry, Graduate School of Medical Sciences, Kumamoto University Hospital, Kumamoto, Japan
[e] Department of Clinical Pharmaceutical Sciences, Graduate School of Pharmaceutical Sciences, Kumamoto University, Japan
[f] Department of Pharmacy, Kumamoto University Hospital, Kumamoto, Japan

ARTICLE INFO

Article history:
Received 13 September 2012
Revised 4 October 2012
Accepted 16 October 2012
Available online 26 October 2012

Edited by Ned Mantei

Keywords:
Transthyretin
Glucagon
Pancreas
Pancreatic alpha cell
Glucose homeostasis

ABSTRACT

Although transthyretin (TTR) is expressed in pancreatic alpha (glucagon) cells in the islets of Langerhans, the function of TTR in pancreatic alpha cells remains unknown. In this study, by using TTR knockout (TTR KO) mice, we determined the novel role of TTR in glucose homeostasis. We demonstrated that TTR KO mice evidenced impaired recovery of blood glucose and glucagon levels. Lack of TTR induced significantly lower levels of glucagon in the islets of Langerhans. These results suggest that TTR expressed in pancreatic alpha cells may play important roles in glucose homeostasis via regulating the expression of glucagon.

1. Introduction

Glucagon, a peptide hormone of 29 amino acids, is synthesized in and secreted from pancreatic alpha cells of the islets of Langerhans in response to mixed nutrient meals, administration of oral or intravenous (i.v.) amino acids, activation of the autonomic nervous system, and hypoglycemia [1,2]. The main action of glucagon is to raise blood glucose levels in response to hypoglycemia by increasing hepatic glycogenolysis and gluconeogenesis [3]. The circulating half-life of immunoreactive glucagon in humans is estimated to be between 5 and 6 min [4]. It is well known that the balance between insulin and glucagon controls glucose homeostasis [5]. Thus, the primary role of glucagon is correcting hypoglycemia caused by malnutrition, fasting, and treatment of diabetes to achieve normoglycemia [6–9]. Insulin treatment in diabetes, especially type 1 diabetes, greatly increases the risk of hypoglycemia, with effects on a number of organs including brain, and causes critical systemic symptoms such as hypoglycemic coma [10–12]. In addition, an absent glucagon response plays a prominent role in a failure to correct hypoglycemia induced by insulin and may exacerbate critical systemic symptoms [8]. Therefore, tight control of glucagon secretion has significant implications for stable glucose homeostasis.

Transthyretin (TTR) is a functional plasma protein, which forms a tetramer composed of four identical subunits, and serves as a transport protein for thyroxine in association with retinol-binding protein [13]. TTR is synthesized predominantly by the liver, which is therefore the main source of TTR in plasma [14,15]. It is well-documented that plasma TTR levels are reduced in inflammatory conditions and in malnutrition caused by surgery or chronic diseases [16–19]. However, TTR is expressed in considerable amounts in the choroid plexus, retinal pigment epithelium, pancreatic alpha and beta cells, although the function of TTR synthesized by these particular cells is largely unknown [20–24]. Certain studies reported a significantly lower plasma TTR level in diabetic patients than in non-diabetic subjects [25,26]. Moreover, in islet beta cells of the pancreas, TTR promoted insulin stimulus-secretion coupling and protected against beta cell apoptosis in type 1 diabetes [27]. In addition, TTR has been shown to be normally expressed in

Abbreviations: qRT-PCR, real-time quantitative RT-PCR; TTR, transthyretin; TTR KO, transthyretin knockout; WT, wild-type; ITT, insulin tolerance test

* Corresponding author. Address: Department of Diagnostic Medicine, Graduate School of Medical Sciences, Kumamoto University, 1-1-1 Honjo, Kumamoto 860-8556, Japan. Fax: +81 96 373 5283.
E-mail address: hjono@fc.kuh.kumamoto-u.ac.jp (H. Jono).

0014-5793/$36.00
http://dx.doi.org/10.1016/j.febslet.2012.10.025

pancreatic alpha cells and stored in secretory vesicles [24]. Moreover, it has also been shown that TTR co-localized with glucagon exactly in pancreatic alpha cells, suggesting that TTR synthesized by pancreatic alpha cells may be involved in glucose homeostasis [24]. However, the biological significances of TTR expressed in pancreatic alpha cells remain unknown.

In view of the evidences provided in previous reports, we hypothesized that TTR may play important roles in glucose homeostasis. In this study, we focused on TTR that is synthesized by pancreatic alpha cells, and we evaluated the possible role of TTR in expression and plasma levels of glucagon during glucose fluctuations.

2. Materials and methods

2.1. Animals

Wild-type (WT) and TTR knockout (TTR KO) mice in the C57BL/6 J background [28], were used in this study. Mice were adult males, each 8–10 weeks old and each weighing 20–25 g. The animals were maintained in a pathogen-free environment at the Center for Animal Resources and Development, Kumamoto University.

2.2. Insulin tolerance test (ITT)

In the ITT, performed after a 3-h fast, human regular insulin (1 IU/kg) was administered intraperitoneally (i.p.) to mice, and the blood glucose level was measured by using an Accu-Chek Inform Blood Glucose Monitoring System (Roche Diagnostics, Indianapolis, IN).

2.3. Fasting conditions and collection of samples

Plasma samples of mice for ELISA were collected at 0, 6, 12, and 24 h after fast. Samples of pancreas and liver for (qRT-PCR) were sharply excised, and then immediately frozen in liquid nitrogen.

2.4. Cells and cell culture

The cell lines PANC-1 (human pancreas epithelioid carcinoma cells), alpha TC1 clone 6 (mouse pancreatic alpha cells), and HepG2 (human hepatocellular carcinoma cells) were obtained from ATCC (Manassas, VA) and were cultured in DMEM (Invitrogen, Grand Island, NY) supplemented with 10% FBS. All cells were grown in 5% CO_2 at 37 °C.

2.5. RNA isolation and qRT-PCR

Total RNA was isolated from each tissue specimen and treated cells by using TRIzol (Invitrogen, Carlsbad, CA), according to the manufacturer's protocol. Total RNA (0.5 μg) was reverse-transcribed to cDNA by using the ExScript RT reagent (Takara Bio Inc., Shiga, Japan) according to the manufacturer's instructions. Each PCR reaction was done with 2 μl of cDNA and 0.2 μM of each primer in a LightCycler System with SYBR Premix Ex Taq (Takara Bio Inc.). Agarose gel electrophoresis was also performed as previously described. The following primers were used: mouse glucagon: forward, 5-TGAATTTGAGAGGCATGCTG-3; reverse, 5-GGTTTGAATCAGCCAGTTGA-3; mouse TTR: forward, 5-CATGAAT TCGCGGATGTG-3; reverse, 5-GATGGTGTAGTGGCGATGG-3; mouse β-actin: forward, 5-TGACAGGATGCAGAAGGAGA-3; reverse, 5-GC TGGAAGGTGGACAGTGAG-3; human TTR: forward, 5-CATTCTTG GCAGGATGGCTTC-3; reverse, 5-CTCCCAGGTGTCATCAGCAG-3; and human glyceraldehyde-3-phosphate dehydrogenase (GAPDH): forward, 5-GCACCGTCAAGGCTGAGAAC-3; reverse, 5-ATGGTGGTG AAGACGCCAGT-3.

2.6. Transfection and fasting in vitro

Cells were cultured in 12 well culture plates (Becton, Dickinson, Franklin Lakes, NJ) at a density of 2×10^5 cells per well, at 37 °C in a humidified atmosphere of 5% CO_2 in air for 48 h. Confluent alpha TC1 clone 6 cells were transfected with two different kinds of siRNA against murine TTR, and PANC-1 cells were transfected with human TTR plasmid by using Lipofectamine 2000 (Invitrogen) according to the manufacturer's protocol. After incubation for 24 or 48 h in serum-free medium, total RNA and protein were isolated. Alpha TC1 clone 6 cells or PANC-1 cells transiently transfected with control siRNA or control vector were used as controls. Chemical siRNA sequences for TTR siRNA1 were as follows: TTR siRNA1 sense strand 5′-CAGUGUUCUUGCUCUAUAATT-3′, TTR siRNA1 antisense strand 5′-UUAUAGAGCAAGAACACUGTT-3′ (Sigma–Aldrich, Tokyo, Japan). For evaluation of the effect of fasting on cells, after cells were incubated in serum-free high-glucose or low-glucose DMEM for 72 h, and thereafter total RNA was isolated.

2.7. Protein extraction form pancreas and pancreatic islets

Protein in the total pancreas and isolated pancreatic islets from mice was obtained by using acid ethanol (15% 1 M HCl, 75% ethanol, 10% H_2O).

2.8. Isolation of pancreatic islets

Mouse pancreatic islets were isolated by means of collagenase digestion. Mice were anesthetized by i.p. with sodium thiopental. Collagenase (collagenase type S-1, 0.6 mg/ml; Nitta Gelatin Inc., Osaka, Japan) was dissolved in Hanks' Balanced Salt Solutions (Sigma–Aldrich) with 800 KIU/ml aprotinin (Wako, Osaka, Japan). The collagenase solution was injected into the common bile duct. Pancreas were dissected and incubated in the collagenase solution at 37 °C for 20 min with shaking. These samples were then mixed with ice-cold isotonic sucrose buffer and were chilled on ice for 20 min. Clarified islets were collected for use in experiments.

2.9. Analysis of glucagon secretion

After being incubated in DMEM for 24 h, 5 groups, for each group contained 15 islets, were incubated for 1 h in Ca^{2+}-containing HEPES-added Krebs–Ringer bicarbonate buffer (HKRB) with 2.2 mM glucose in 5% CO_2 at 37 °C, followed by test incubation for 1 h in HKRB with 2.2 or 22 mM glucose.

2.10. Immunohistochemical staining

Paraffin-embedded 4-μm-thick sections were prepared and deparaffinized in xylene and rehydrated in graded alcohols. Slides were treated with periodic acid for 10 min at room temperature, after which they were incubated in 5% normal serum for 1 h at room temperature in a moist chamber. For immunohistochemical staining of glucagon, a polyclonal rabbit anti-glucagon antibody (Cell Signaling Technology, Danvers, MA), diluted 1:100 in dilution buffer, served as the primary antibody. Rabbit anti-mouse TTR antiserum, diluted 1:50 in dilution buffer, served as the primary antibody for mouse TTR. The secondary antibody was an HRP-conjugated goat anti-rabbit immunoglobulin antibody (Dako, Glostrup, Denmark) diluted 1:100 in buffer. The dilution buffer was 0.5% Bovine serum albumin (BSA). Reactivity was visualized via the DAB Liquid System (Dako), according to the manufacturer's instructions. Sections were counterstained with hematoxylin.

2.11. ELISA

The glucagon concentration in plasma, extracts of total pancreas and islets from mice, and cell lines was measured by using the Rat Glucagon ELISA Kit (Wako), according to the manufacturer's instructions for undiluted plasma samples, 1000 times dilution of extracts of pancreas and islets, 500 times dilution of cell supernatants, and 50 times dilution of cell lysates.

2.12. Statistics

Data were expressed as means ± S.D. and ±S.E.M., according to the previous study [29]. Controls and treated groups were compared by using Student's *t* test. The accepted level of significance was $P < 0.05$.

3. Results

3.1. Change in blood glucose levels in WT and TTR KO mice during the ITT

RT-PCR confirmed expression of TTR mRNA in the pancreas of mice (Fig. 1A). In sections of pancreatic tissues, TTR was expressed in all islets from WT mice, with cells showing a preferential peripheral distribution, but islets from TTR KO mice evidenced no TTR expression (Fig. 1A). ITT showed that the blood glucose level in WT mice started to recover at 30 min after the insulin injection (Fig. 1B). However, those in TTR KO mice decreased sharply by 60 min after the injection compared with the baseline of the blood glucose level. Furthermore, TTR KO mice had continuously suppressed blood glucose levels compared with WT mice at 60, 90, 120, and 180 min after the insulin injection (Fig. 1B). We assumed that the impaired plasma glucagon levels caused the sharp decrease of the blood glucose levels in the ITT.

3.2. Plasma glucagon levels in WT and TTR KO mice in the ITT and during fasting

We next investigated plasma glucagon levels in WT and TTR KO mice. As Fig. 2A shows, although WT mice showed higher plasma glucagon levels after the insulin injection, TTR KO mice showed a much smaller increase in plasma glucagon levels in a time-dependent manner after the injection. In addition, in sections of pancreatic tissues from WT and TTR KO mice at 20 min after the insulin injection, almost all of the islets from WT mice demonstrated strong glucagon immunoreactivity, but islets from TTR KO mice showed only weak immunoreactivity (Fig. 2B). Furthermore, we compared plasma glucagon levels between WT and TTR KO mice during chronic glucose fluctuations induced by fasting. As seen in Fig. 2C, consistent with the results of the ITT, TTR KO mice showed significantly lower plasma glucagon level by fasting. In contrast to the glucagon levels, no significant difference of plasma insulin levels between WT and TTR KO mice was observed (Fig. S1).

3.3. Glucagon content in pancreatic islets from WT and TTR KO mice

We next determined the glucagon content in pancreatic islets from WT and TTR KO mice. Under normal conditions, pancreatic islets from WT mice demonstrated a strong positive immunoreactivity for glucagon, with a preferential distribution in the periphery (Fig. 3A). Pancreatic islets from TTR KO mice, however, showed a much weaker positive reaction (Fig. 3A). The quantitative analysis showed that in TTR KO mice, the glucagon content in the total pancreas was significantly lower than that for WT mice, *i.e.*, about 10% of the glucagon content of WT mice (Fig. 3B). To confirm these results, pure pancreatic islets were isolated and analyzed. As seen in Fig. 3C, similar to the results for the total pancreas, the glucagon content in islets isolated from TTR KO mice was about 50% of that in from WT mice.

3.4. Glucagon secretion from pancreatic islets isolated from TTR KO mice

To confirm the results obtained from *in vivo* experiments, glucagon secretion from pure pancreatic islets-isolated from WT and TTR KO mice were analyzed. Transfer from high-glucose condition to low-glucose condition has been shown to induce glucagon secretion from pancreatic islets. In our study, performed under similar conditions, pancreatic islets from WT mice showed

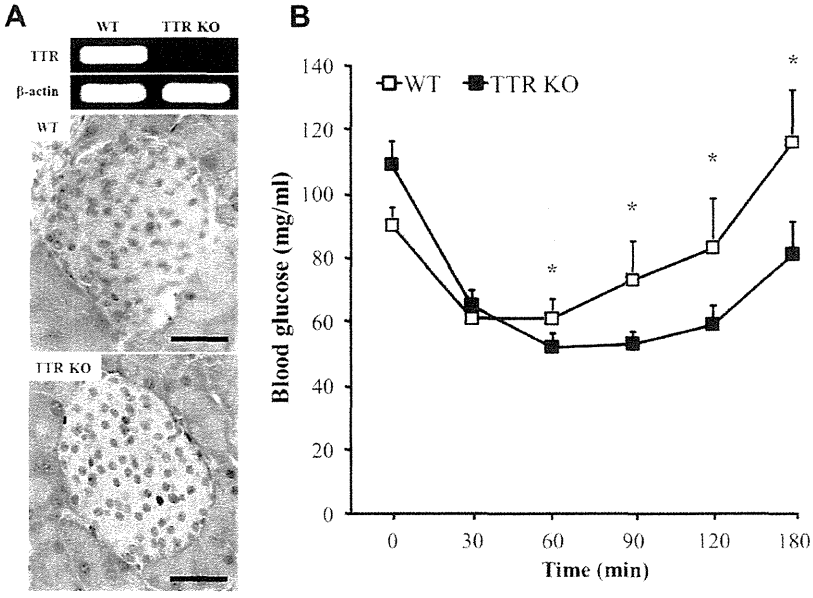

Fig. 1. TTR expression in pancreatic tissues of mice and changes in blood glucose levels in WT and TTR KO mice during the ITT. (A) Expression of TTR mRNA in the pancreas of mice (top panel); TTR expression in islets from WT mice, with cells showing a preferential peripheral distribution (middle panel), but no TTR expression in TTR KO mice (bottom panel). Scale bars = 100 μm. (B) Mice received human regular insulin (1 IU/kg i.p.), and the serum glucose level was monitored at 0, 30, 60, 90, 120, and 180 min (mean ± S.E.M.). $n = 6$. $^*P < 0.05$.

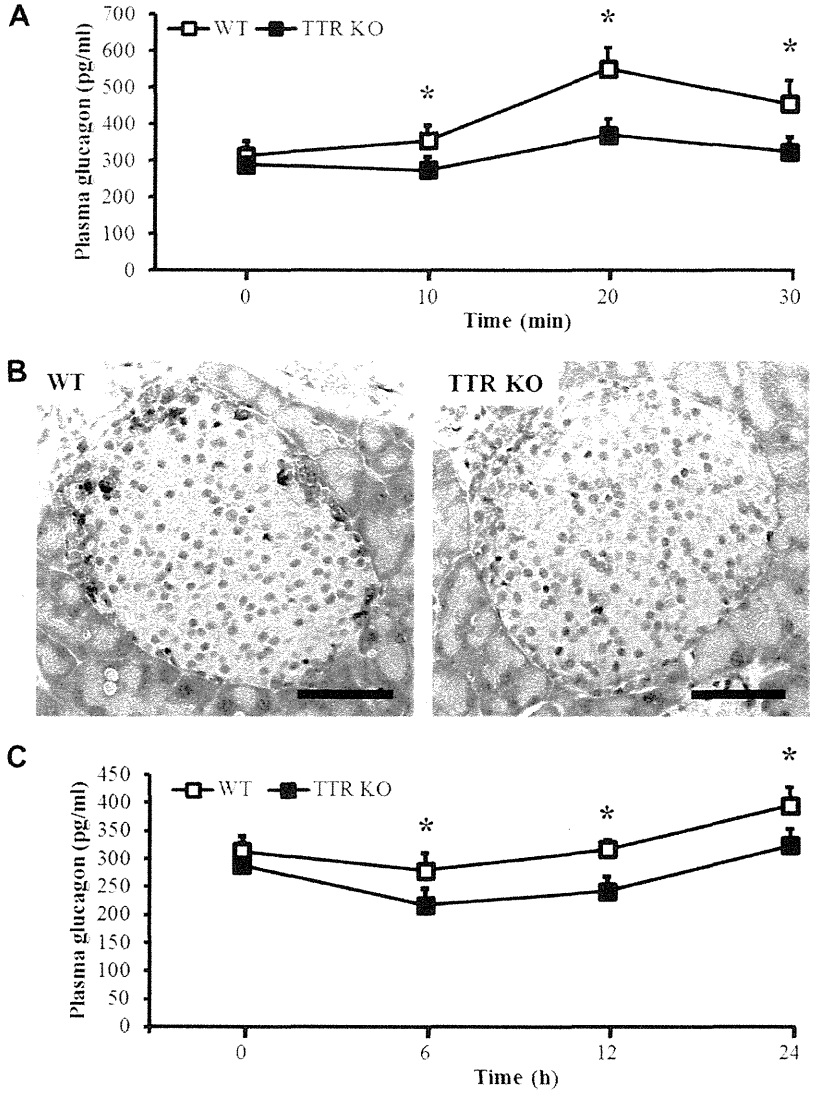

Fig. 2. Plasma glucagon levels in WT and TTR KO mice in the ITT and during fasting. (A) Mice underwent the ITT, and plasma glucagon was measured at 0, 10, 20, and 30 min by using ELISA (mean ± S.E.M.). $n = 10$. (B) Examples of pancreatic islets from mice after the ITT. At 20 min after ITT, immunohistochemistry revealed high-intensity glucagon staining in pancreatic islets from WT mice (left) and low-intensity glucagon staining in pancreatic islets from TTR KO mice (right). Scale bars = 100 μm. (C) Mice were fasted for 24 h, and plasma glucagon was measured by ELISA at 0, 6, 12, and 24 h (mean ± S.E.M.). $n = 11$. $^*P < 0.05$.

increased glucagon secretion in the low-glucose compared with the high-glucose condition. In addition, islets from TTR KO mice had glucagon levels similar to those of WT mice in the high-glucose condition. However, no increase in glucagon level was observed in the islets from TTR KO mice in response to the low-glucose condition, in contrast to WT mice. The glucagon levels in the islets from TTR KO mice were significantly lower than those from WT mice under low-glucose conditions (Fig. 4A). We also evaluated the glucagon contents remaining in pancreatic islets after glucagon secretion. Pancreatic islets from TTR KO mice showed a significantly lower level of glucagon than islets from WT mice-only about 40% of the WT level (Fig. 4B). Because the TTR KO islets showed the lower glucagon content, we assumed that the content of glucagon was impacted by the decrease of glucagon expression.

3.5. Changes in glucagon expression as related to TTR expression

We next determined glucagon mRNA levels after 12 h of fasting. Expression of glucagon mRNA in the total pancreas from TTR KO mice was significantly lower than that from WT mice (Fig. 5A). While, no obvious alteration was seen in insulin mRNA expression (Fig. S2). In addition, downregulation of TTR expression by two different sequences of TTR siRNA led to a significant reduction in glucagon expression in alpha TC1 clone 6 cells at both mRNA andprotein levels (Fig. 5B, Figs. S3 and S4). In contrast, overexpression of WT-TTR by using the TTR plasmid significantly increased glucagon mRNA expression in PANC-1 cells (Fig. 5C).

3.6. Starvation-induced changes in pancreatic TTR expression

Previous reports demonstrated that TTR levels decreased during progressive malnutrition and that this effect was linked to expression of TTR in the liver, the main organ of production of TTR circulating in the blood [17]. In our study, as expected, expression of TTR in the liver from WT mice significantly decreased. In contrast, expression of TTR in the total pancreas from WT mice markedly increased, about 2.5 times, during starvation induced by fasting for 24 h (Fig. 6a and b). Similar to the results obtained from *in vivo* experiments, HepG2 cells, a liver cell line, showed a marked reduction in TTR expression after incubation under low-glucose

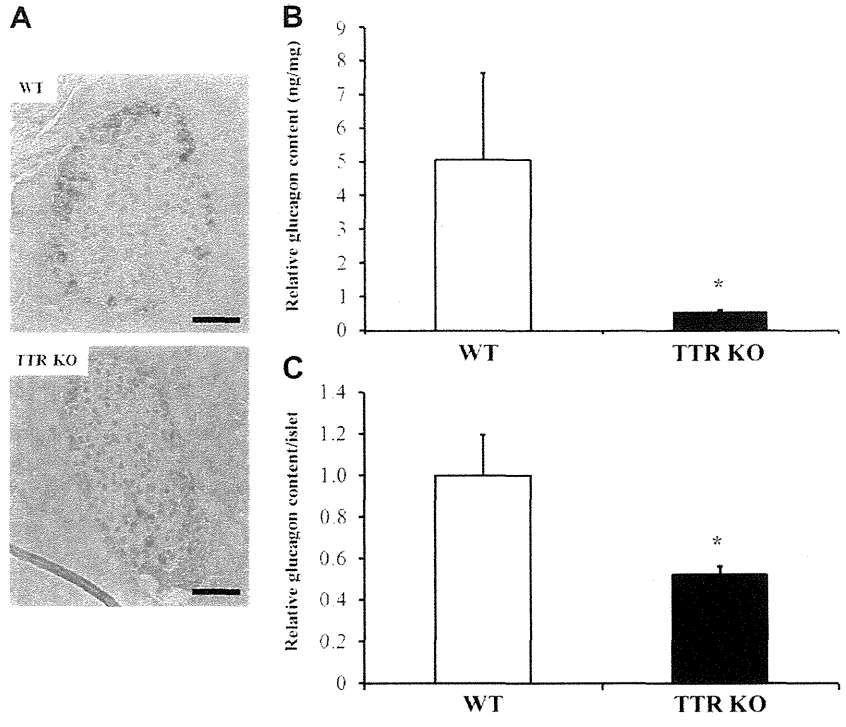

Fig. 3. Glucagon content in pancreatic islets from WT and TTR KO mice. (A) An example of high-intensity glucagon staining in pancreatic islets from WT mice (top) and low-intensity glucagon staining in pancreatic islets from TTR KO mice (bottom). Scale bars = 100 μm. (B) Glucagon content in the total pancreas from WT and TTR KO mice as measured by ELISA (mean ± S.D.). $n = 6$. (C) Glucagon content in isolated pancreatic islets from WT and TTR KO mice, as measured by ELISA (mean ± S.D.). $n = 3$. $^{*}P < 0.05$.

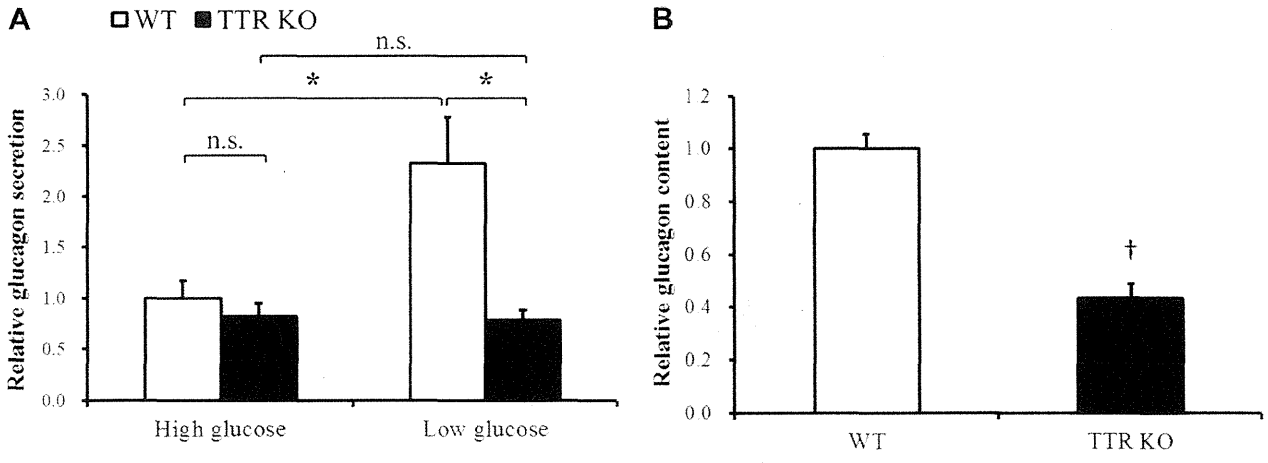

Fig. 4. Glucagon secretion from pancreatic islets from WT and TTR KO mice. (A) Pancreatic islets isolated from WT and TTR KO mice were incubated under high- (22 mM) or low- (2.2 mM) glucose condition. Glucagon levels were assessed by ELISA (mean ± S.E.M.). $n = 5$. $^{*}P < 0.05$. n.s., not significant. (B) Remaining glucagon contents in isolated pancreatic islets from WT and TTR KO mice after glucagon secretion after incubation in low-glucose condition, as measured by ELISA (mean ± S.E.M.). $n = 5$. $^{\dagger}P < 0.01$.

conditions for 72 h. However, alpha TC1 clone 6 cells evidenced significantly increased glucagon mRNA expression after incubation in glucose-poor medium for 48 h (Fig. 6c and d).

4. Discussion

A previous report suggests that, on the basis of electron microscopic evidence, TTR in pancreatic islets is mainly expressed in pancreatic alpha cells and is stored in secretory vesicles [24]. In the present study, we demonstrated that TTR KO mice, compared with WT mice, evidenced impaired blood glucose recovery and plasma glucagon levels during both acute and chronic glucose fluctuations. These results were confirmed by using isolated pancreatic islets from WT and TTR KO mice. These interesting phenomena suggest that TTR plays important roles in glucose homeostasis during glucose fluctuations, especially periods of low blood glucose levels, by regulating the amount of glucagon secreted.

One interesting finding of this study is that the lack of TTR reduced the plasma glucagon level during both acute and chronic glucose fluctuations. Glucagon and insulin constitute part of a feedback system that keeps blood glucose levels stable. The reduced glucagon level destroys the balance between insulin and glucagon, and affects the stability of blood glucose levels. These effects may be amplified by injections of insulin used to treat insulin-dependent diabetes, or by long periods of malnutrition. The pancreas releases glucagon when blood glucose levels fall too low,

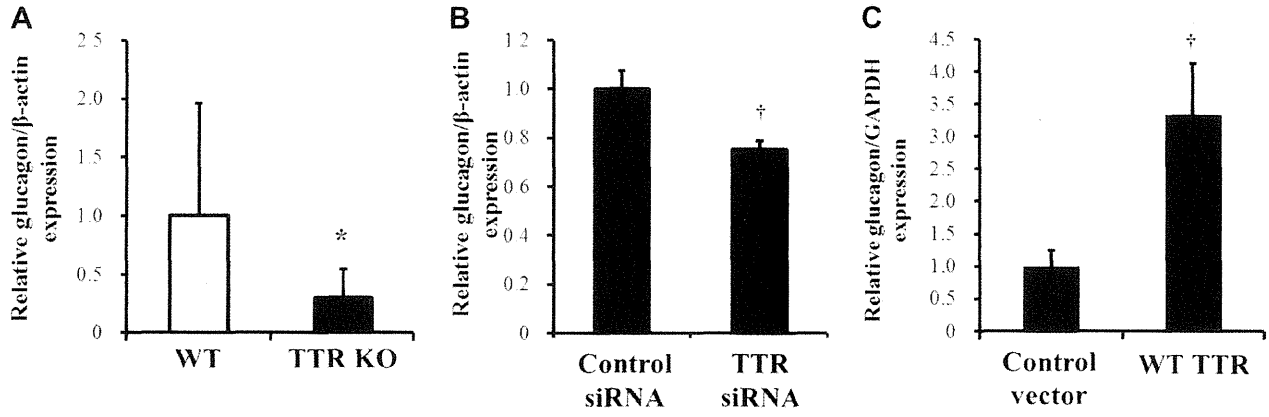

Fig. 5. Effects of TTR on glucagon expression. (A) Mice were fasted for 12 h, and glucagon mRNA expression was measured by means of qRT-PCR (mean ± S.D.). $n = 14$. (B) effect of blocking TTR signaling on glucagon mRNA expression in alpha TC1 clone 6 cells. Blocking was achieved by using TTR siRNA (100 nM) (mean ± S.D.). $n = 3$. (C) Effect of TTR overexpression on glucagon mRNA expression in PANC-1 cells. Overexpression was achieved by using TTR plasmid (0.3 μg) (mean ± S.D.). $n = 3$. $^{*}P < 0.05$; $^{\dagger}P < 0.01$.

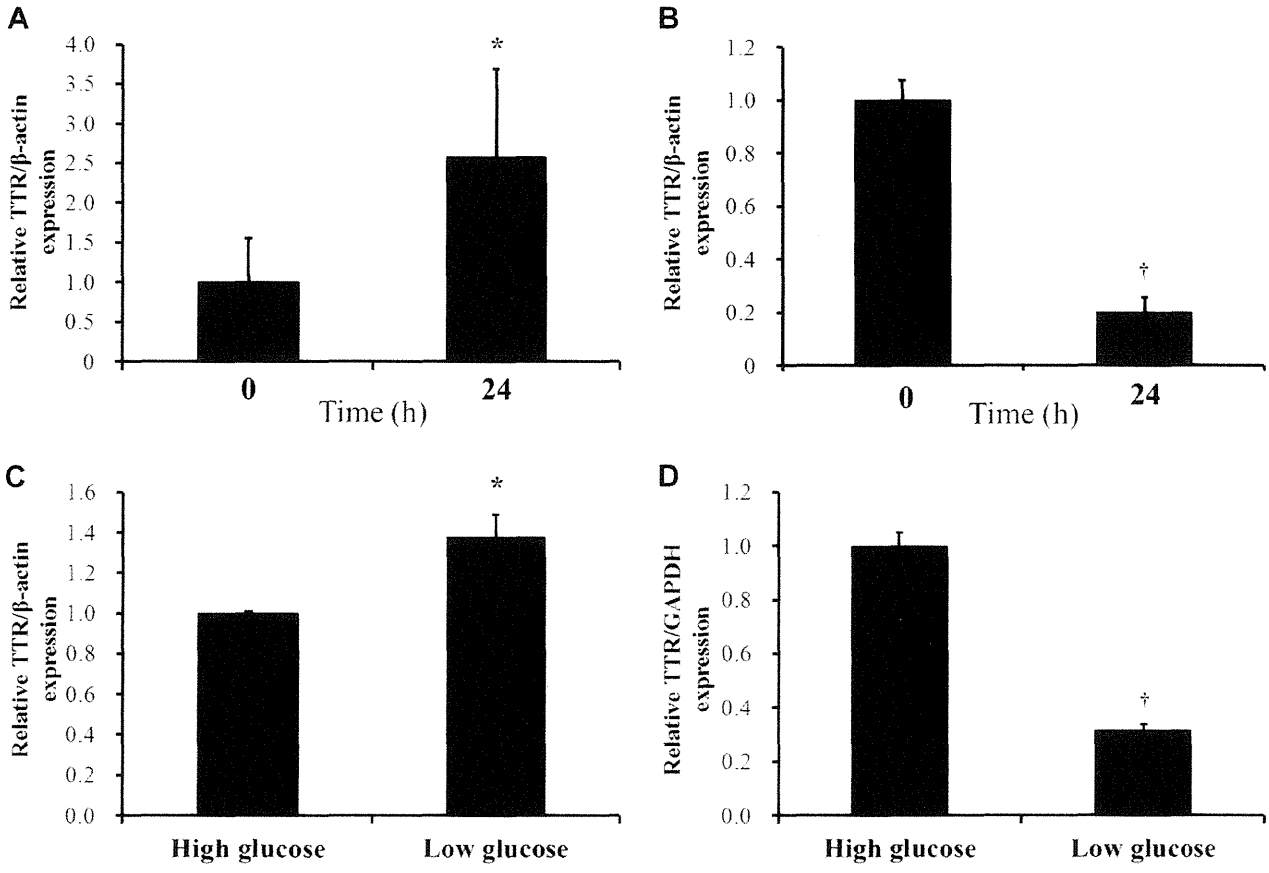

Fig. 6. Effects of starvation on TTR expression in pancreas and liver. WT mice were fasted for 24 h, and TTR mRNA expression in pancreas (A) and liver (B) was measured by means of qRT-PCR (mean ± S.D.). (C) and (D) alpha TC1 clone 6 (C) or HepG2 (D) cells were incubated under high- or low-glucose condition for 72 h. TTR mRNA expression was measured by means of qRT-PCR (mean ± S.D.). $n = 3$. $^{*}P < 0.05$; $^{\dagger}P < 0.01$.

and glucagon facilitates the liver's conversion of stored glycogen into glucose, which is released into the bloodstream. Low plasma glucagon levels cause a failure in the relief of acute or chronic severe hypoglycemia, which affects many important organs and major physiological functions [6]. Especially, because neurons cannot use other energy sources such as fatty acids to any great degree, brain depends absolutely on glucose as a fuel [30]. Thus, rapid response and dynamic glucagon secretion when blood glucose levels are low is extremely important for maintenance of glucose homeostasis. Our data suggest that TTR performs a novel function and plays important roles in stabilizing blood glucose levels via control of glucagon. It should be noted that, despite the well-known fact that glucagon concentration is regulated by insulin concentration, no obvious difference in plasma insulin levels was observed between WT and TTR KO mice (Fig. S1). These data suggest that TTR in pancreatic alpha cells played an important role to increase

the plasma glucagon levels during glucose fluctuations. A conditional TTR KO mouse which lack TTR only in pancreas may help confirming these findings. Our future studies will focus on more precise determination of the roles of TTR in glucose homeostasis.

In the present study, we found that TTR KO mice showed a significantly lower glucagon content compared with WT mice, and we found a similar phenomenon in the *in vitro* studies using pancreatic islets. It should be noticed that the similar numbers of pancreatic islets in whole pancreas of WT and TTR KO mice were observed by microscope (average number of WT: 32 ± 6/field; TTR KO: 28 ± 4/field). Moreover, we found that glucagon mRNA expression in pancreatic cell lines had a high positive association with the level of TTR expression. These results suggest that the lack of TTR impaired the accumulation or storage of glucagon in pancreatic alpha cells, and we considered that the reduced contents of glucagon could be caused by the decrease of mRNA levels. As shown in Figs. 1 and 2, by ITT, plasma glucagon levels 20 min post-injection were lower in TTR KO than WT, and significant differences were noted from 60 min in blood glucose level. These results suggest that because pancreatic alpha cells rapidly secrete abundant glucagon in response to hypoglycemia, and since the half-life of glucagon is relatively short, 5–6 min [4], the lack of TTR may reduce the level of glucagon mRNA, which in turn leads to the deficiency of plasma glucagon levels for insulin antagonistic activity. Although the role of TTR in glycogenolysis in liver has yet to be determined, TTR may serve as one of the enhancers of glucagon expression after acute secretion of glucagon in pancreatic alpha cells. Also, we previously reported that glucose metabolism is impaired in familial amyloidotic polyneuropathy, which is caused by mutated TTR, in which amyloid deposition commonly occurs in the pancreas [31]. Previous reports demonstrated that glucagon gene expression is tightly controlled by various transcription factors, such as Pax6, Foxa1, Foxa2, and MafB/cMaf [2,32,33]. Of these transcription factors, Foxa2 (also called hepatic nuclear factor-3) is known to be essential for strong expression of TTR gene in the liver [34,35]. It should be noted that Pax6 mRNA expression was significantly reduced by TTR knockdown with siRNA in alpha TC1 clone 6 cells (Fig. S5). These lines of evidence suggest that TTR in pancreatic alpha cells may also be controlled by various transcription factors, such as Pax6 and Foxa2, in response to hypoglycemia and may serve as a mediator of up-regulation of glucagon expression. In addition to the glucagon contents, because TTR is stored in secretory vesicles [24], TTR may affect the secretion of glucagon. Moreover, since we also found that the expression levels of insulin was also affected, but not obviously, by the lack of TTR (Fig. S2), further investigation is needed to explain in detail the mechanism underlying cross-talk between glucagon and TTR expression in glucose homeostasis. In addition, instead of normal cells, we used alpha TC1 clone6 and PANC-1 cell lines to obtain supportive evidence (Figs. 5 and 6). Unlike normal pancreatic alpha cells, alpha TC1 clone 6 cells express the high levels of glucagon by the control of the rat preproglucagon promoter and terminally differentiated. PANC-1 is an epithelioid carcinoma cell line derived from human pancreas and secret the low levels of hormones. Our future studies will focus on more precise determination by using the normal pancreatic alpha cells of the roles of TTR in glucose.

Other interesting findings of this study are that, different from the situation in the liver, hypoglycemia that was induced by insulin injections and fasting significantly enhanced TTR expression in pancreatic alpha cells, and starvation produced a similar result. These findings suggest that TTR expression may be controlled by specific transcriptional regulation in pancreatic alpha cells as described above, which differ from hepatic cells. We will clarify the mechanism in the future study.

In conclusion, unlike liver that synthesize TTR, the pancreas expresses TTR by means of a distinct mechanism. In addition to the well-known function of TTR, such as transporting thyroxine in association with retinol-binding protein, TTR that is expressed in pancreatic alpha cells may play important roles in glucose homeostasis during glucose fluctuations by regulating glucagon expression.

Acknowledgments

The authors thank Hiroko Katsura for technical assistance. This work was supported in part by the Advanced Education Program for Integrated Clinical, Basic and Social Medicine, Graduate School of Medical Sciences, Kumamoto University (Program for Enhancing Systematic Education in Graduate Schools, MEXT, Japan). The authors' work was supported by grants from the Amyloidosis Research Committee; the Pathogenesis, Therapy of Hereditary Neuropathy Research Committee; the Surveys and Research on Specific Diseases from the Ministry of Health and Welfare of Japan; and Research for the Future Program Grant and Grants-in-Aid for Scientific Research (B) 20253742 from the Ministry of Education, Science, Sports and Culture of Japan. This work was also supported in part by the scholarship for the Graduate School of Medical Sciences, Kumamoto University, Japan.

Appendix A. Supplementary data

Supplementary data associated with this article can be found, in the online version, at http://dx.doi.org/10.1016/j.febslet.2012.10.025.

References

[1] Dunning, B.E. and Gerich, J.E. (2007) The role of alpha-cell dysregulation in fasting and postprandial hyperglycemia in type 2 diabetes and therapeutic implications. Endocr. Rev. 28, 253–283.
[2] Gromada, J., Franklin, I. and Wollheim, C.B. (2007) Alpha-cells of the endocrine pancreas: 35 years of research but the enigma remains. Endocr. Rev. 28, 84–116.
[3] Jiang, G. and Zhang, B.B. (2003) Glucagon and regulation of glucose metabolism. Am. J. Physiol. Endocrinol. Metab. 284, 671–678.
[4] Alford, F.P., Bloom, S.R. and Nabarro, J.D. (1976) Glucagon metabolism in man. Studies on the metabolic clearance rate and the plasma acute disappearance time of glucagon in normal and diabetic subjects. J. Clin. Endocrinol. Metab. 42, 830–838.
[5] Aronoff, S.L., Berkowitz, K., Shreiner, B. and Want, L. (2004) Glucose metabolism and regulation: beyond insulin and glucagon. Diabetes Spectr. 17, 183–190.
[6] Cryer, P.E. (1993) Glucose counterregulation: prevention and correction of hypoglycemia in humans. Am. J. Physiol. Endocrinol. Metab. 264, 149–155.
[7] Bosco, D., Armanet, M., Morel, P., Niclauss, N., Sgroi, A., Muller, Y.D., Giovannoni, L., Parnaud, G. and Berney, T. (2010) Unique arrangement of alpha- and beta-cells in human islets of Langerhans. Diabetes 59, 1202–1210.
[8] Cryer, P.E., Davis, S.N. and Shamoon, H. (2003) Hypoglycemia in diabetes. Diabetes Care 26, 1902–1912.
[9] Asplin, C.M., Paquette, T.L. and Palmer, J.P. (1981) *In vivo* inhibition of glucagon secretion by paracrine beta cell activity in man. J. Clin. Invest. 68, 314–318.
[10] Ben-Ami, H., Nagachandran, P., Mendelson, A. and Edoute, Y. (1999) Drug-induced hypoglycemic coma in 102 diabetic patients. Arch. Intern. Med. 159, 281–284.
[11] Bending, J.J., Pickup, J.C. and Keen, H. (1985) Frequency of diabetic ketoacidosis and hypoglycemic coma during treatment with continuous subcutaneous insulin infusion. Audit of medical care. Am. J. Med. 79, 685–691.
[12] Holleman, F., Schmitt, H., Rottiers, R., Rees, A., Symanowski, S. and Anderson, J.H.The Benelux-UK Insulin Lispro Study Group (1997) Reduced frequency of severe hypoglycemia and coma in well-controlled IDDM patients treated with insulin Lispro. Diabetes Care 20, 1827–1832.
[13] Raz, A. and Goodman, D.S. (1969) The interaction of thyroxine with human plasma prealbumin and with the prealbumin-retinol-binding protein complex. J. Biol. Chem. 244, 3230–3237.
[14] Maeda, S., Mita, S., Araki, S. and Shimada, K. (1986) Structure and expression of the mutant prealbumin gene associated with familial amyloidotic polyneuropathy. Mol. Biol. Med. 3, 329–338.
[15] Ando, Y. (2005) Liver transplantation and new therapeutic approaches for familial amyloidotic polyneuropathy (FAP). Med. Mol. Morphol. 38, 142–154.
[16] Weeke, B. and Jarnum, S. (1971) Serum concentration of 19 serum proteins in Crohn's disease and ulcerative colitis. Gut 12, 297–302.

[17] Ingenbleek, Y., De Visscher, M. and De Nayer, P. (1972) Measurement of prealbumin as index of protein–calorie malnutrition. Lancet 2, 106–109.
[18] Ingenbleek, Y. and Young, V.R. (2002) Transthyretin (prealbumin) in health and disease: nutritional implications. Annu. Rev. Nutr. 14, 495–533.
[19] Raguso, C.A., Genton, L., Dupertuis, Y.M. and Pichard, C. (2002) Assessment of nutritional status in organ transplant: is transthyretin a reliable indicator? Clin. Chem. Lab. Med. 40, 1325–1328.
[20] Aleshire, S.L., Bradley, C.A., Richardson, L.D. and Parl, F.F. (1983) Localization of human prealbumin in choroid plexus epithelium. J. Histochem. Cytochem. 31, 608–612.
[21] Cavallaro, T., Martone, R.L., Dwork, A.J., Schon, E.A. and Herbert, J. (1990) The retinal pigment epithelium is the unique site of transthyretin synthesis in the rat eye. Invest. Ophthalmol. Vis. Sci. 31, 497–501.
[22] Kawaji, T., Ando, Y., Nakamura, M., Yamamoto, K., Ando, E., Takano, A., Inomata, Y., Hirata, A. and Tanihara, H. (2005) Transthyretin synthesis in rabbit ciliary pigment epithelium. Exp. Eye Res. 81, 306–312.
[23] Jacobsson, B., Pettersson, T., Sandstedt, B. and Carlström, A. (1979) Prealbumin in the islets of Langerhans. IRCS Med. Sci. 7, 590.
[24] Westermark, G.T. and Westermark, P. (2008) Transthyretin and amyloid in the islets of Langerhans in type-2 diabetes. Exp. Diabetes Res. Article ID 429274.
[25] Itoh, N., Hanafusa, T., Miyagawa, J., Tamura, S., Inada, M., Kawata, S., Kono, N. and Tarui, S. (1992) Transthyretin (prealbumin) in the pancreas and sera of newly diagnosed type I (insulin-dependent) diabetic patients. J. Clin. Endocrinol. Metab. 74, 1372–1377.
[26] Tuitoek, P.J., Ziari, S., Tsin, A.T., Rajotte, R.V., Suh, M. and Basu, T.K. (1996) Streptozotocin-induced diabetes in rats is associated with impaired metabolic availability of vitamin A (retinol). Br. J. Nutr. 75, 615–622.
[27] Refai, E., Dekki, N., Yang, S.N., Imreh, G., Cabrera, O., Yu, L., Yang, G., Norgren, S., Rössner, S.M., Inverardi, L., Ricordi, C., Olivecrona, G., Andersson, M., Jörnvall, H., Berggren, P.O. and Juntti-Berggren, L. (2005) Transthyretin constitutes a functional component in pancreatic beta-cell stimulus-secretion coupling. Proc. Natl. Acad. Sci. USA 102, 17020–17025.
[28] Episkopou, V., Maeda, S., Nishiguchi, S., Shimada, K., Gaitanaris, G.A., Gottesman, M.E. and Robertson, E.J. (1993) Disruption of the transthyretin gene results in mice with depressed levels of plasma retinol and thyroid hormone. Proc. Natl. Acad. Sci. USA 90, 2375–2379.
[29] Cumming, G., Fidler, F. and Vaux, D.L. (2007) Error bars in experimental biology. J. Cell Biol. 177, 7–11.
[30] Cunnane, S., Nugent, S., Roy, M., Courchesne-Loyer, A., Croteau, E., Tremblay, S., Castellano, A., Pifferi, F., Bocti, C., Paquet, N., Begdouri, H., Bentourkia, M., Turcotte, E., Allard, M., Barberger-Gateau, P., Fulop, T. and Rapoport, S.I. (2011) Brain fuel metabolism, aging, and Alzheimer's disease. Nutrition 27, 3–20.
[31] Ando, Y., Yi, S., Nakagawa, T., Ikegawa, S., Hirota, M., Miyazaki, A. and Araki, S. (1991) Disturbed metabolism of glucose and related hormones in familial amyloidotic polyneuropathy: hypersensitivities of the autonomic nervous system and therapeutic prevention. J. Auton. Nerv. Syst. 35, 63–70.
[32] Jin, T. (2008) Mechanisms underlying proglucagon gene expression. J. Endocrinol. 198, 17–28.
[33] Huang, H.P. and Tsai, M.J. (2000) Transcription factors involved in pancreatic islet development. J. Biomed. Sci. 7, 27–34.
[34] Samadani, U., Qian, X. and Costa, R.H. (1996) Identification of a transthyretin enhancer site that selectively binds the hepatocyte nuclear factor-3 beta isoform. Gene Expr. 6, 23–33.
[35] Costa, R.H., Kalinichenko, V.V., Holterman, A.X. and Wang, X. (2003) Transcription factors in liver development, differentiation, and regeneration. Hepatology 38, 1331–1347.

OPEN ACCESS Freely available online

PLOS ONE

A Pilot Investigation of Visceral Fat Adiposity and Gene Expression Profile in Peripheral Blood Cells

Masaya Yamaoka[1], Norikazu Maeda[1]*, Seiji Nakamura[2], Susumu Kashine[1], Yasuhiko Nakagawa[1], Aki Hiuge-Shimizu[1], Kohei Okita[1], Akihisa Imagawa[1], Yuji Matsuzawa[3], Ken-ichi Matsubara[2], Tohru Funahashi[1], Iichiro Shimomura[1]

1 Department of Metabolic Medicine, Graduate School of Medicine, Osaka University, Suita, Osaka, Japan, **2** DNA Chip Research Inc., Yokohama, Kanagawa, Japan, **3** Sumitomo Hospital, Osaka, Osaka, Japan

Abstract

Evidence suggests that visceral fat accumulation plays a central role in the development of metabolic syndrome. Excess visceral fat causes local chronic low-grade inflammation and dysregulation of adipocytokines, which contribute in the pathogenesis of the metabolic syndrome. These changes may affect the gene expression in peripheral blood cells. This study for the first time examined the association between visceral fat adiposity and gene expression profile in peripheral blood cells. The gene expression profile was analyzed in peripheral blood cells from 28 obese subjects by microarray analysis. Reverse transcription-polymerase chain reaction (RT-PCR) was performed using peripheral blood cells from 57 obese subjects. Obesity was defined as body mass index (BMI) greater than 25 kg/m^2 according to the Japanese criteria, and the estimated visceral fat area (eVFA) was measured by abdominal bioelectrical impedance. Analysis of gene expression profile was carried out with Agilent whole human genome 4×44 K oligo-DNA microarray. The expression of several genes related to circadian rhythm, inflammation, and oxidative stress correlated significantly with visceral fat accumulation. Period homolog 1 (PER1) mRNA level in blood cells correlated negatively with visceral fat adiposity. Stepwise multiple regression analysis identified eVFA as a significant determinant of PER1 expression. In conclusion, visceral fat adiposity correlated with the expression of genes related to circadian rhythm and inflammation in peripheral blood cells.

Citation: Yamaoka M, Maeda N, Nakamura S, Kashine S, Nakagawa Y, et al. (2012) A Pilot Investigation of Visceral Fat Adiposity and Gene Expression Profile in Peripheral Blood Cells. PLoS ONE 7(10): e47377. doi:10.1371/journal.pone.0047377

Editor: Reury F.P Bacurau, University of Sao Paulo, Brazil

Received May 14, 2012; **Accepted** September 11, 2012; **Published** October 16, 2012

Funding: This work was supported in part by Grants-in-Aid for Scientific Research (C) no. 22590979 (to N.M.) and Scientific Research on Innovative Areas no. 22126008 (to T.F.). The funders had no role in study design, data collection and analysis, decision to publish, or preparation of the manuscript.

Competing Interests: The authors have read the journal's policy and have the following conflicts: one or more of the authors are employed by a commercial company DNA Chip Research Inc. This does not alter the authors' adherence to all PLOS ONE policies on sharing data and materials.

* E-mail: norikazu_maeda@endmet.med.osaka-u.ac.jp

Introduction

It has been shown that there is a significant association between computed tomography (CT)-based fat distribution and life style-related diseases, such as diabetes, dyslipidemia, and hypertension. Visceral fat-related obesity is closely associated with the development of atherosclerotic diseases [1]. The metabolic syndrome is strongly linked to visceral fat adiposity. The exact pathomechanisms of the metabolic syndrome are not clear at present but seem to involve accumulation of macrophages in adipose tissue, which induce a state of chronic low-grade inflammation by producing a battery of inflammatory mediators. In addition, these macrophages interact with adipocytes through free fatty acids and adipocytokines, creating a vicious cycle that promotes the development of the metabolic syndrome and atherosclerosis [2–4]. However, to date, there is no method to evaluate the function and condition of human visceral fat.

A series of recent studies demonstrated that the adipose tissue of obese subjects contains not only macrophages but also non-macrophage immunocytes, such as T-cells [5,6], B-cells [7], and eosinophils [8], and that these cells accelerate the development of metabolic syndrome. These evidences imply that gene expression profile in peripheral blood cells may reflect the visceral fat condition. However, there is no report demonstrating the relation of peripheral blood gene expressions and visceral fat accumulation. Hence, the present study tested the association between visceral fat adiposity and the gene expression profile in peripheral blood cells to search novel surrogate markers relating to visceral fat adiposity and to establish novel diagnostic tools for metabolic syndrome.

Materials and Methods

Study Population

All subjects were inpatients of the Division of Endocrinology & Metabolism, Osaka University Hospital, Osaka. Written informed consent was obtained from each subject after explaining the purpose and potential complications of the study. The study protocol was approved by the human ethics committee of Osaka University and the study was registered with the University hospital Medical Information Network (Number: UMIN 000001663). Obesity was defined as body mass index (BMI) greater than 25 kg/m^2 [9]. Subjects with type 1 diabetes mellitus, autoimmune diseases, malignant diseases, and infectious diseases were excluded from the study. Patients treated with statins and/or thiazolidinediones were also excluded. Sixty-two subjects were

enrolled in the study, although five subjects were later excluded due to RNA degradation in the blood samples collected from these individuals. Thus, the present study was conducted in 57 obese patients.

Clinical Parameters

The estimated visceral fat area (eVFA) was measured by abdominal bioelectrical impedance analysis (BIA), as reported previously [10,11]. Physical examination and collection of blood samples were conducted on the same day. The homeostasis model−assessment of insulin resistance (HOMA-IR) was calculated by the equation: HOMA-IR = fasting insulin (μU/mL) x fasting glucose (mg/dL)/405.

The intima-media thickness (IMT) of the carotid arteries was measured using a high-resolution B-mode ultrasonography system (Xario; Toshiba Medical Systems Corp., Tochigi, Japan) with an electrical linear transducer (mid-frequency 7.5 MHz). IMT represented the distance between two parallel echogenic lines corresponding to the blood-intima and media-adventitia interfaces on the posterior wall of the artery. Three determinations of IMT were conducted at the site of the thickest point, maximum IMT (max-IMT) and two adjacent points (located 1 cm upstream and 1 cm downstream from this site). These three determinations were averaged and expressed as the mean IMT.

Type 2 diabetes mellitus was defined as fasting plasma glucose (FPG) concentration ≥126 mg/dL, 2-h plasma glucose concentration following 75 g oral glucose load of ≥200 mg/dL, or treatment with glucose-lowering agents. Hypertension was defined as systolic blood pressure (BP) ≥140 mmHg, diastolic BP≥90 mmHg, or treatment with anti-hypertensive agents. Dyslipidemia was defined as fasting triglycerides (TG) ≥150 mg/dL, high-density lipoprotein cholesterol (HDL-C) <40 mg/dL, or low-density lipoprotein cholesterol (LDL-C) ≥140 mg/dL, or treatment with lipid-lowering agents.

Isolation of RNA

For total RNA isolation, blood samples were collected into PaxGene Blood RNA tubes (PreAnalytiX/QIAGEN Inc., Valencia, CA) at 7:30 am and left to stand for 2 h at room temperature. The blood samples in the PaxGene Blood RNA tubes were stored at −20°C for 2 days and subsequently kept at −80°C until analysis. Total RNA was extracted by using PaxGene Blood RNA Kit (PreAnalytiX/QIAGEN) according to the protocol supplied by the manufacturer.

Microarray Analysis

After RNA was qualified by the Agilent 2100 Bioanalyzer, 250 ng of total RNA was converted to cDNA, amplified, and labeled with Cy3-labeled CTP using the Quick Amp Labeling kit (Agilent Technologies, Santa Clara, CA) according to the protocol supplied by the manufacturer. Following labeling and clean up, the amplified RNA and dye incorporation were quantified using a ND-1000 Spectrophotometer (Nano Drop Technologies, Wilmington, DE) and hybridized to Agilent whole human genome 4 × 44 K oligo-DNA microarray (Agilent Technologies, Santa Clara, CA). After hybridization, the arrays were washed consecutively by using Gene Expression Wash Pack (Agilent Technologies). Fluorescence images of the hybridized arrays were generated using the Agilent DNA Microarray Scanner, and the intensities were extracted with Agilent Feature Extraction software ver.10.7.3.1. The raw microarray data are deposited in the National Center for Biotechnology Information Gene Expression Omnibus (GEO Series GSE28038).

Real-Time RT-PCR

First-strand cDNA was synthesized from 180 ng of total RNA using Thermoscript RT (Invitrogen, Carlsbad, CA) and oligo dT primer. Real-time quantitative PCR amplification was conducted with the LightCycler 1.5 (Roche Diagnostics, Tokyo, Japan) using LightCycler-FastStart DNA Master SYBR Green I (Roche Diagnostics, Tokyo, Japan) according to the protocol recommended by the manufacturer. The final result for each sample was normalized to the respective GAPDH (glyceraldedyde-3-phosphate dehydrogenase) value. The primer sets used were: PER1, 5′-GAACTCAGATGTGGCTAGACC-3′ and 5′-TGTCAGCAACTTTGTCCAGGG-3′; GAPDH, 5′-AAGGGCATCCTGGGCTACA-3′ and 5′-GAGGAGTGGGTGTCGCTGTTG-3′.

Microarray Data Analyses

The raw microarray intensities were processed by the percentile shift method (75th percentile) using the GeneSpring GX11 (Agilent Technologies) so as to normalize the range of expression intensities for inter-microarray. Only those genes whose expression data were available in more than 50% of hybridizations were included for further analyses. The normalized data were exported from the GeneSpring GX software. The correlation between peripheral blood gene expression levels and Log-eVFA levels was examined by Pearson's correlation under the R environment (http://cran.at.r-project.org). Gene Ontology (GO) information was retrieved from the annotations in GeneSpring GX11.

Clinical Data Analysis

Geometric mean values were used for insulin and C-reactive protein (CRP) due to the skewed distribution of the data. Non-normally distributed variables were log-transformed before analysis. The Spearman rank correlation coefficients for the study population as a whole were analyzed for Log-eVFA levels and other clinical variables. A P values less than 0.05 denoted the presence of significant difference. Pearson's correlation coefficient was used to examine the relationship between period homolog 1 (PER1) and metabolic parameters. Stepwise multiple regression analysis with backward stepwise elimination was conducted to identify those parameters that significantly contributed to PER1. Log-eVFA, HOMA-IR, WBC and CRP were entered as independent variables in the analysis. All calculations were performed using the JMP software (JMP 9.0; SAS Institute Inc., Cary, NC). Data are expressed as mean±SD.

Results

Characteristics of the Subjects

The clinical characteristics of the participating subjects are listed in the Table 1. The mean BMI and eVFA of 57 patients were 30.6 kg/m^2 (range, 25.4–51.2 kg/m^2) and 166.8 cm^2 (range, 80–386 cm^2), respectively. The mean HOMA-IR was 3.0, reflecting mild insulin resistance. The proportion of patients with diabetes mellitus, dyslipidemia, and hypertension was 75%, 73%, and 57%, respectively. Frequency of patients treated with lipid-lowering drugs, anti-hypertensive drugs, oral glucose-lowering agents, insulin, and sleeping drugs was 25%, 42%, 18%, 42%, and 28%, respectively.

Serum adiponectin concentrations correlated inversely with eVFA (Figure S1A) while CRP levels correlated positively with eVFA (Figure S1B). Insulin concentrations correlated significantly with eVFA (Figure S1C) and HOMA-IR tended to increase in parallel with increase in eVFA (Figure S1D). The leukocyte count, but not the erythrocyte count or platelet count, correlated

Table 1. Characteristics of participants.

N	57
Age (years)	51.7±13.5
Male/Female	27.0/30
Body weight (kg)	79.4±16.7
BMI (kg/m^2)	30.6±5.3
Waist circumference (cm)	100.7±12.5
eVFA (cm^2)	166.8±164.4
Log-eVFA	2.2±0.15
Systolic blood pressure (mmHg)	128.8±14.9
Diastolic blood pressure (mmHg)	76.3±10.9
Fasting glucose (mg/dL)	139.6±50.3
Hemoglobin A1c (%)	8.1±2.2
Immunoreactive insulin (μU/ml)	12.1±5.8
HOMA-IR (unit)	3.0±1.3
Total cholesterol (mg/dL)	210.4±37.1
LDL-C (mg/dL)	134.1±33.3
HDL-C (mg/dL)	46.8±10.2
Triglyceride (mg/dL)	155.7±76.8
Creatinine (mg/dL)	0.8±0.29
Ureic acid (mg/dL)	6.2±1.5
Serum adiponectin (μg/mL)	6.7±4
WBC (/μL)	6758.0±1838
Neutrophils (%)	55.2±7.5
Lymphocytes (%)	35.8±8
Eosinophils (%)	3.0±1.5
Basophils (%)	0.6±0.9
Monocytes (%)	7.4±7.5
RBC (×10^4/μL)	466.0±53
Platelet (×10^4/μL)	23.4±5.6
CRP (mg/dL)	0.4±0.48
Diabetes mellitus, n (%)	43 (75)
Dyslipidemia, n (%)	42 (73)
Hypertention, n (%)	33 (57)
Mean IMT (mm)	0.9±0.25
Medication	
Oral glucose-lowering drugs, n (%)	10 (18)
Insulin, n (%)	24 (42)
Lipid lowering drugs, n (%)	14 (26)
Antihypertensive drugs, n (%)	24 (42)

Data are mean ± SD. BMI; body mass index, eVFA; estimated visceral fat area, LDL-C; low density lipoprotein-cholesterol, HDL-C; high density lipoprotein-cholesterol, HOMA-IR; homeostasis model assessment of insulin resistance, IMT; imtima-media thickness.

doi:10.1371/journal.pone.0047377.t001

significantly with eVFA (Figure S2A to S2C). Furthermore, the lymphocyte, monocyte, and neutrophil counts, but not those of eosinophils and basophils, correlated positively with eVFA (Figure S2D to S2H).

Analysis of Gene Expression Profiles

Peripheral blood RNA samples from 28 subjects (BMI 31.9±6.0 kg/m^2, VFA 199.4±89.4 cm^2) were subjected to microarray analysis. The target probes were selected under the condition that significant signals were detected in more than 14 cases and thus 27969 genes were extracted for gene expression analysis. Table 2 lists the top 20 genes that correlated significantly with eVFA: 8 genes correlated positively and 12 genes correlated negatively with eVFA. Among these genes, the solute carrier family 46 member 3 (SLC46A3), which is classified as a membrane protein, showed the highest statistical significance with eVFA ($P = 0.000006$). Importantly, significant correlations with eVFA were also observed in genes related to oxidative stress and inflammation, such as peroxiredoxin 3 (PRDX3) ($P = 0.00033$), suppressor of cytokine signaling 3 (SOCS3) ($P = 0.0007$), and ORAI calcium release-activated calcium modulator 1 (ORAI1) ($P = 0.0009$). Interestingly, a negative correlation with eVFA was observed in period homolog 1 (PER1), which is classified as a transcription factor and recognized as a circadian clock gene ($P = 0.0011$).

Next, we conducted gene ontology (GO) analysis and searched for genes involved in circadian rhythm (GO:0007623), inflammation (GO:0006954), oxidative stress (GO:0006979), immune response (GO:0006955), lipid metabolism (GO:0006629), and glucose metabolism (GO:0006006). Figure 1A shows the prevalence of genes that showed significant correlation with eVFA. The number of circadian rhythm genes was small, but 5 genes (18.5%) showed significant correlation with eVFA. The frequencies of inflammation-, oxidative stress-, and immune response-related genes that correlated significantly with eVFA were 5.9%, 7.8%, and 8.8%, respectively. Furthermore, the frequencies of lipid metabolism- and glucose metabolism-related genes that correlated

Table 2. Correlation coefficients of peripheral blood cell gene expression with visceral fat adiposity.

Gene Symbol	Gene Name	P value
Positively correlated genes		
SLC46A3	solute carrier family 46, member 3	0.000006
DUSP3	dual specificity phosphatase 3	0.00007
DEF8	differentially expressed in FDCP 8 homolog	0.0002
APOM	apolipoprotein M	0.00033
PRDX3	peroxiredoxin 3	0.00033
SOCS3	suppressor of cytokine signaling 3	0.0007
LOC644538	hypothetical protein LOC644538	0.0007
DOK4	docking protein 4	0.0011
Negatively correlated genes		
TSGA14	testis specific, 14	0.00002
CABIN1	calcineurin binding protein 1	0.00007
ZFP36	zinc finger protein 36	0.0001
RAB37	RAB37, member RAS oncogene family	0.0002
PBXIP1	pre-B-cell leukemia homeobox interacting protein 1	0.00032
RABGAP1L	RAB GTPase activating protein 1-like	0.0004
SMPD1	sphingomyelin phosphodiesterase 1, acid lysosomal	0.0004
ZNF174	zinc finger protein 174	0.0006
C3orf16	chromosome 3 open reading frame 16	0.0006
CCND3	cyclin D3	0.0007
ORAI1	ORAI calcium release-activated calcium modulator 1	0.0009
PER1	period homolog 1	0.0011

doi:10.1371/journal.pone.0047377.t002

significantly with eVFA were 3.0% and 6.1%, respectively. Increasing evidence demonstrates a close relationship between the disturbance of circadian clock oscillator and the development of metabolic syndrome [12–14]. Table 3 shows gene probes related to circadian rhythm (GO:0007623). PER1, v-erb-b2 erythroblastic leukemia viral oncogene homolog 3 (ERBB3), clock homolog (CLOCK), prokineticin 2 (PROK2), and cryptochrome 2 (CRY2) correlated significantly with eVFA.

Association between PER1 and Metabolic Parameters

As shown in Figure 1A and Table 3, genes relating to circadian rhythm were highly correlated with eVFA. The highest correlation with eVFA was observed in PER1 among them. RT-PCR was, therefore, performed in 57 subjects to revalue the association of eVFA and PER1 mRNA levels in peripheral blood cells. As shown in Figure 1B, PER1 mRNA levels correlated negatively with eVFA (Figure 1B).

Table 4 lists the correlation coefficients for the relationship between PER1 and various metabolic parameters. Age- and sex-adjusted univariate analysis showed that PER1 correlated negatively with log-eVFA, HOMA-IR, WBC, and CRP. Stepwise multiple regression analysis revealed log-eVFA as a significant determinant of PER1.

Discussion

The main findings of the present study were: *(1)* Visceral fat adiposity correlated with the expression of various genes related to circadian rhythm, inflammation, and oxidative stress, in peripheral blood cells. *(2)* Peripheral blood PER1 mRNA expression level correlated negatively with visceral fat area. *(3)* Visceral fat area

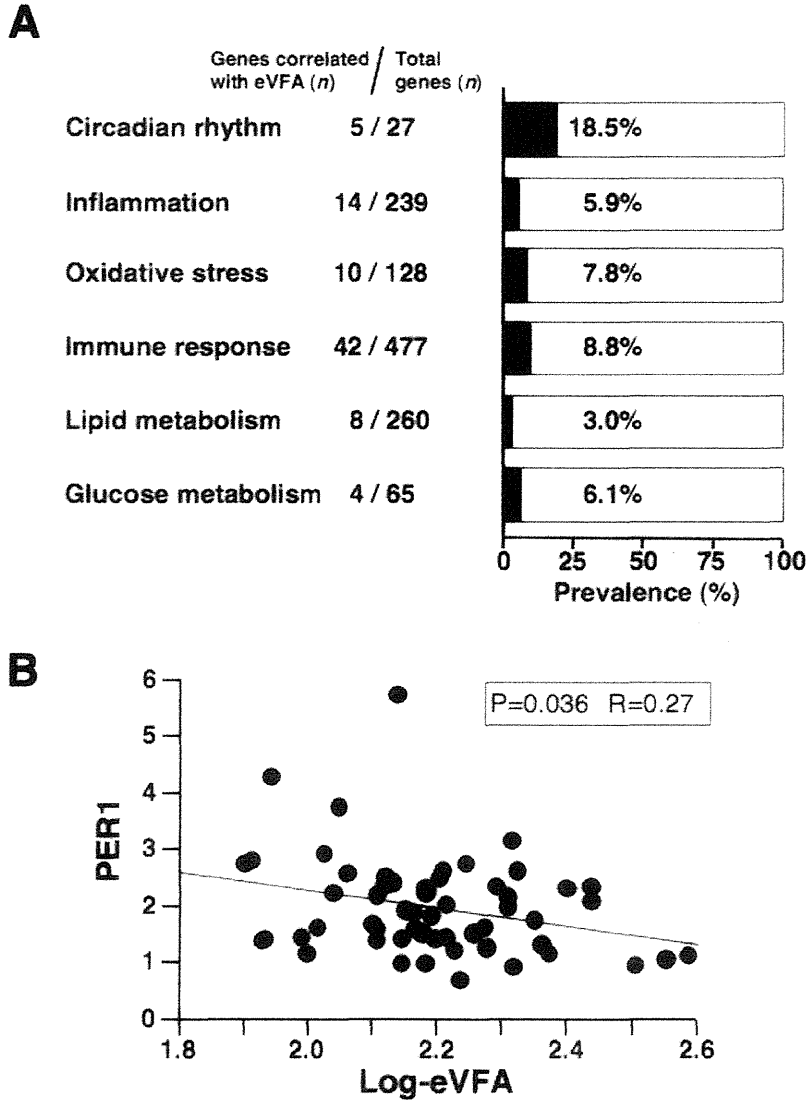

Figure 1. Gene expression profile in peripheral blood cells. (A) Prevalence of gene probes correlated with estimated visceral fat area (eVFA). Gene ontology analysis was performed based on the microarray data. (B) Correlation between PER1 mRNA level and eVFA. Total RNAs from peripheral blood cells of 57 subjects were subjected to RT-PCR.
doi:10.1371/journal.pone.0047377.g001